

Supporting Information

Impact of human serum albumin on Cu^{II} and Zn^{II} complexation by ATSM (diacetyl-bis(N4- methylthiosemicarbazone) and a water soluble analogue

Álvaro Martínez-Camarena^{a,b*}, Angélique Sour,^b Peter Faller^{b,c}

a) ICMol, Departament de Química Inorgànica, Universitat de València, C/ Catedrático José Beltrán 2, 46980, Paterna, Spain. E-mail: alvaro.martinez@uv.es

b) Institut de Chimie, UMR 7177, Université de Strasbourg, CNRS, 4 Rue Blaise Pascal, 67000 Strasbourg, France.

c) Institut Universitaire de France (IUF), 1 rue Descartes, 75231 Paris, France

Contents

I. Figures

Figure S1. $^1\text{H-NMR}$ spectrum of the ATSM in d_6 -DMSO.

Figure S2. $^1\text{H-NMR}$ spectrum of the 1 in d_6 -DMSO.

Figure S3. $^1\text{H-NMR}$ spectrum of the 2 in d_6 -DMSO.

Figure S4. $^1\text{H-NMR}$ spectrum of the ATSM(CH₂)₃COOH in d_6 -DMSO.

Figure S5. $^{13}\text{C-NMR}$ spectrum of the ATSM(CH₂)₃COOH in d_6 -DMSO.

Figure S6. (A) Experimental (top) and theoretical (bottom) LC-MS spectra of ATSM(CH₂)₃COOH. (B) Detail of the experimental (top) and theoretical (bottom) spectra.

Figure S7. UV-vis spectra of a 30 μM of ATSM in HEPES buffer (pH 7.4, 50 mM) with % of DMSO ranging from 70 (blue) to 0.9 (orange).

Figure S8. UV-vis spectra of a 30 μM of ATSM(CH₂)₃COOH in HEPES buffer (pH 7.4, 50 mM) with % of DMSO ranging from 75 (blue) to 1.7 (orange).

Figure S9. Evolution of the absorbance spectra with time of solutions containing 30 μM of ATSM in HEPES buffer (pH 7.4, 50 mM) with different percentages of DMSO: (A) 1%, (B) 10%, (C) 20% and (D) 30%.

Figure S10. (A) Evolution of the spectra with time of solutions containing 30 μM of ATSM(CH₂)₃COOH and (B) intensity of absorbance at 326 nm in function of time. Medium: HEPES buffer (pH 7.4, 50 mM) with 1% of DMSO.

Figure S11. (A) Evolution of the spectra of solutions containing 30 μM of ATSM in HEPES buffer (pH 7.4, 50 mM) and 70% of DMSO upon addition of aliquots of Cu^{II} and (B) representation of the intensity of absorbance at 470 nm of the solutions in function of [Cu^{II}]/[ATSM].

Figure S12. (A) Evolution of the spectra of solutions containing 30 μM of ATSM(CH₂)₃COOH in HEPES buffer (pH 7.4, 50 mM) and 70% of DMSO upon addition of aliquots of Cu^{II} and (B) representation of the intensity of absorbance at 470 nm of the solutions in function of [Cu^{II}]/[ATSM(CH₂)₃COOH].

Figure S13. UV-vis spectra of a 30 μM of ATSM in presence of Cu^{II} (1 eq) in HEPES buffer (pH 7.4, 50 mM) with % of DMSO ranging from 70 (blue) to 0.9 (orange).

Figure S14. UV-vis spectra of a 30 μM of ATSM(CH₂)₃COOH in presence of Cu^{II} (1 eq) in HEPES buffer (pH 7.4, 50 mM) with % of DMSO ranging from 75 (blue) to 1.7 (orange).

Figure S15. Evolution of the absorbance spectra with time of solutions containing 30 μM of ATSM in presence of Cu^{II} (1 eq) in HEPES buffer (pH 7.4, 50 mM) with different percentages of DMSO: (A) 1%, (B) 10%, (C) 20% and (D) 30%. Insets: intensity of absorbance at 456 nm in function of time.

Figure S16. (A) Evolution of the spectra with time of solutions containing 30 μM of ATSM(CH₂)₃COOH in presence of Cu^{II} (1 eq) and (B) intensity of absorbance at 454 nm in function of time. Medium: HEPES buffer (pH 7.4, 50 mM) with 1% of DMSO.

Figure S17. (A) Evolution of the spectra with time of a 30 μM solution of Cu^{II}-ATSM to which 1 eq of HSA was added and (B) intensity of absorbance at 454 nm in function of time. Medium: HEPES buffer (pH 7.4, 50 mM) with 1% of DMSO.

Figure S18. (A) Evolution of the spectra with time of a 30 μM solution of Cu^{II} -ATSM(CH_2)₃COOH to which 1 eq of HSA was added and (B) intensity of absorbance at 460 nm in function of time. Medium: HEPES buffer (pH 7.4, 50 mM) with 1% of DMSO.

Figure S19. (A) Evolution of the spectra with time of a 30 μM solution of Cu^{II} -HSA to which 1 eq of ATSM(CH_2)₃COOH was added and (B) intensity of absorbance at 460 nm in function of time. Medium: HEPES buffer (pH 7.4, 50 mM) with 1% of DMSO.

Figure S20. Comparative of the spectra of a 30 μM ATSM(CH_2)₃COOH solution (dotted orange line), a 30 μM ATSM(CH_2)₃COOH solution containing 1 eq of Cu^{II} (in dark orange) and a 30 μM ATSM(CH_2)₃COOH solution containing 1 eq of Cu^{II} and 1 eq of HSA (in dark green).

Figure S21. (A) Evolution of the spectra with time of a 30 μM solution of ATSM to which 1 eq of HSA was added and (B) intensity of absorbance at 323 nm in function of time. Medium: HEPES buffer (pH 7.4, 50 mM) with 1% of DMSO.

Figure S22. Comparative of the spectra of a 30 μM ATSM solution (in pale orange), in presence of 1 eq of Cu^{II} (in dark orange) or in presence of 1 eq of Zn^{II} (in dark blue). Medium: HEPES buffer (pH 7.4, 50 mM) with 70% of DMSO.

Figure S23. Comparative of the spectra of a 30 μM ATSM(CH_2)₃COOH solution (in pale orange), in presence of 1 eq of Cu^{II} (in dark orange) or in presence of 1 eq of Zn^{II} (in dark blue). Medium: HEPES buffer (pH 7.4, 50 mM) with 70% of DMSO.

Figure S24. (A) Evolution of the spectra with time of a 30 μM solution of ATSM and Zn^{II} (1:1) after the addition of 1 eq of HSA, (B) intensity of absorbance at 408 nm in function of time. Medium: HEPES buffer (pH 7.4, 50 mM) with 1% of DMSO.

Figure S25. (A) Evolution of the spectra with time of a 30 μM solution of ATSM(CH_2)₃COOH and Zn^{II} (1:1) after the addition of 1 eq of HSA, (B) intensity of absorbance at 423 nm in function of time. Medium: HEPES buffer (pH 7.4, 50 mM) with 1% of DMSO.

Figure S26. (A) Evolution of the spectra with time of a 30 μM solution of HSA and Zn^{II} (1:1) after the addition of 1 eq of ATSM, (B) intensity of absorbance of this solution at 408 nm in function of time, (C) evolution of the spectra with time of a 30 μM solution of HSA and Zn^{II} (1:2) after the addition of 1 eq of ATSM, (D) intensity of absorbance of this solution at 408 nm in function of time. Medium: HEPES buffer (pH 7.4, 50 mM) with 1% of DMSO.

Figure S27. (A) Evolution of the spectra with time of a 30 μM solution of HSA and Zn^{II} (1:1) after the addition of 1 eq of ATSM(CH_2)₃COOH, (B) intensity of absorbance of this solution at 414 nm in function of time, (C) evolution of the spectra with time of a 30 μM solution of HSA and Zn^{II} (1:2) after the addition of 1 eq ATSM(CH_2)₃COOH, (D) intensity of absorbance of this solution at 414 nm in function of time. Medium: HEPES buffer (pH 7.4, 50 mM) with 1% of DMSO.

Figure S28. (A) Comparison between the addition of HSA to a solution of Zn^{II} -ATSM(CH_2)₃COOH (orange) and the addition of ATSM(CH_2)₃COOH to a solution of Zn^{II} -HSA (green), $[\text{ATSM}(\text{CH}_2)_3\text{COOH}] = [\text{HSA}] = [\text{Zn}^{\text{II}}] = 30 \mu\text{M}$, dotted lines correspond to spectra at time 0, and continuous lines correspond to spectra at time 150 min. (B) Intensity of absorbance at 423 nm for the addition of HSA to a solution of Zn^{II} -ATSM(CH_2)₃COOH (orange), the addition of ATSM to a solution of Zn^{II} -HSA (1:1) (dark green) and the addition of ATSM(CH_2)₃COOH to a solution of Zn^{II} -HSA (2:1) (pale green). Medium: HEPES buffer (pH 7.4, 50 mM) 1% of DMSO.

Figure S29. (A) Spectra of a 30 μM solution of Cu^{II} -ATSM after addition of 0.1 to 100 eq of Zn^{II} and (B) intensity of absorbance at 460 nm in function of the equivalents of Zn^{II} (scale in logarithmic units). Medium: HEPES buffer (pH 7.4, 50 mM) with 1% of DMSO.

Figure S30. (A) Spectra of a 30 μM solution of Cu^{II} -ATSM(CH_2)₃COOH after addition of 0.1 to 100 eq of Zn^{II} and (B) intensity of absorbance at 460 nm in function of the equivalents of Zn^{II} (scale in logarithmic units). Medium: HEPES buffer (pH 7.4, 50 mM) with 1% of DMSO.

Figure S31. (A) Evolution of the spectra with time of a 30 μM solution of Cu^{II} -ATSM(CH_2)₃COOH after the addition of 1 eq. of HSA and 10 eq. of Zn^{II} , (B) intensity of absorbance at 460 nm in function of time. Medium: HEPES buffer (pH 7.4, 50 mM) with 1% of DMSO.

Figure S32. (A) Evolution of the spectra with time of a 30 μM solution of Cu^{II} - Zn^{II} -HSA after the addition of 1 eq of ATSM, (B) intensity of absorbance at 421 nm (in blue) and at 458 nm (in yellow) in function of time. Medium: HEPES buffer (pH 7.4, 50 mM) with 1% of DMSO.

Figure S33. (A) Evolution of the spectra with time of a 30 μM solution of Cu^{II} - Zn^{II} -HSA after the addition of 1 eq of ATSM(CH_2)₃COOH, (B) intensity of absorbance at 423 nm (in blue) and at 461 nm (in yellow) in function of time. Medium: HEPES buffer (pH 7.4, 50 mM) with 1% of DMSO.

Figure S34. (A) Detail of the evolution of the spectra with time of a 30 μM solution of Cu^{II} - Zn^{II} -HSA after the addition of 1 eq of ATSM(CH_2)₃COOH, (B) intensity of absorbance of the ligand (322 nm, orange), the Zn^{II} complex (421 nm, blue) and the Cu^{II} complex (458 nm, yellow) in function of time. Medium: HEPES buffer (pH 7.4, 50 mM) with 1% of DMSO.

Figure S35. Evolution of the absorbance spectra with time of a 30 μM solution of Cu^{II} -ATSM after the addition of 1 eq. of EDTA in HEPES buffer (pH 7.4, 50 mM) with different percentages of DMSO: (A) 1%, (B) 10%, (C) 20% and (D) 30%.

Figure S36. (A) Evolution of the absorbance spectra with time of a 30 μM solution of Cu^{II} -ATSM(CH_2)₃COOH after the addition of 1 eq. of EDTA during 2.5 h, (B) intensity of absorbance of this solution at 408 nm in function of time and (C) and (D) the equivalent measurements carried out during 500 h. Medium: HEPES buffer (pH 7.4, 50 mM) with 1% of DMSO.

Figure S37. (A) Evolution of the spectra with time of a 30 μM solution of Cu^{II} -ATSM after the addition of 1 eq. of HSA and 1 eq. of EDTA, (B) intensity of absorbance at 480 nm in function of time. Medium: HEPES buffer (pH 7.4, 50 mM) with 1% of DMSO.

Figure S38. (A) Evolution of the spectra with time of a 30 μM solution of Cu^{II} -EDTA after the addition of 1 eq. of HSA and 1 eq. of ATSM, (B) intensity of absorbance at 322 nm in function of time. Medium: HEPES buffer (pH 7.4, 50 mM) with 1% of DMSO.

Figure S39. (A) Evolution of the spectra with time of a 30 μM solution of Cu^{II} after the addition of 1,000 eq. of EDTA and then 1 eq. of ATSM(CH_2)₃COOH, (B) intensity of absorbance at 325 nm (in blue) and at 453 nm (in yellow) in function of time vs. the competition with 1 eq. of EDTA (325 nm in pale blue and 453 nm in pale yellow). Medium: HEPES buffer (pH 7.4, 50 mM) with 1% of DMSO.

Figure S40. (A) Evolution of the spectra with time of a 30 μM solution of Cu^{II} -ATSM(CH_2)₃COOH after the addition of 1,000 eq. of EDTA, (B) intensity of absorbance at 325 nm (in blue) and at 453 nm (in yellow) in function of time vs. the competition with 1 eq. of EDTA (325 nm in pale blue and 453 nm in pale yellow). Medium: HEPES buffer (pH 7.4, 50 mM) with 1% of DMSO.

II. Tables

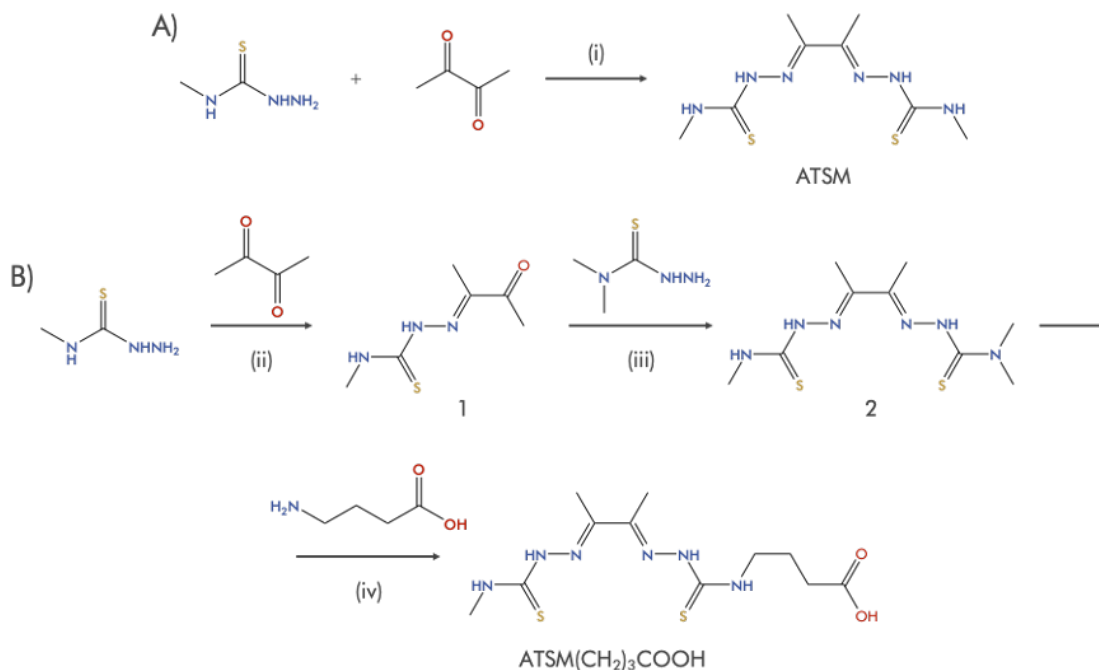
Table 1. Distances and angles in the complex $\text{Cu}^{\text{II}}\text{-ATSM}$

Table 2. Distances and angles in the complex $\text{Cu}^{\text{II}}\text{-ATSM}(\text{CH}_2)_3\text{COOH}$

III. References

I. SYNTHESIS OF THE LIGANDS

The synthesis of the two semicarbazone ligands ATSM and ATSM(CH₂)₃COOH was carried out following the procedures previously described, depicted in Scheme 1.^{3,4,27} The characterisation of the compounds is depicted in Figures S1-S6.



Scheme 1. Scheme of the synthetic routes for (A) ATSM and (B) ATSM(CH₂)₃COOH. Conditions: (i) EtOH, glacial AcOH; reflux, 5h; yield 40 %; (ii) HCl, H₂O; at 3 °C, 2 h; yield 88 %; (iii) DMF, room temperature, 48 h; yield 81 %; and (iv) CH₃CN; reflux, 41 h; yield 48 %.

Synthesis of diacetylbis(4-methyl-3-thiosemicarbazone) (ATSM)^{3,4}

A solution containing 4-methyl-3-thiosemicarbazide (1.048 g, 9.97 mmol) in 10 mL of absolute EtOH was mixed with a solution of 2,3-butanedione (0.439 g, 5.10 mmol) in 5 mL of absolute EtOH. Then, 6 drops of glacial acetic acid were added, and the mixture was refluxed under Ar for 5 h. After cooling, the resulting suspension was left overnight at 4 °C and then it was filtered. The obtained solid was washed with abundant warm EtOH and diethyl ether. ATSM (0.517 g, yield 40 %) was obtained as a pale yellow powder. ¹H NMR (400 MHz, DMSO-*d*₆), δ (ppm): 10.20 (s, 2H), 8.36 (s, 2H), 3.03 (s, 3H), 3.02 (s, 3H), 2.20 (s, 6H).

Synthesis of diacetyl-*mono*-4-methyl-3-thio-semicarbazone (1)²⁷

10 drops of HCl 37 % were added to a suspension containing 2,3-butadione (2.40 g, 27.9 mmol) in 50 mL of distilled water. The solution was cooled down to 3 °C, 4-methyl-3-thiosemicarbazide (2.65 g, 25.2 mmol) was added in small fractions for 1.5 h and under intense stirring. The suspension was stirred for 40 minutes more at 3 °C. Then, the suspended solid was extracted with CHCl₃ (3 × 100 mL), the organic phases were combined and dried with MgSO₄, and the solvent was evaporated under reduced pressure. The resulting pale-yellow solid was recrystallised with n-pentane (60 mL) in presence of 1 mL of CHCl₃. After filtration and washing with pentane, compound 1 was obtained as a pale-yellow powder (3.83 g, yield 87.9 %). ¹H NMR (400.13 MHz, DMSO-*d*₆), δ (ppm): 10.61 (s, 1H), 8.61 (s, 1H), 3.06 (s, 3H), 2.42 (s, 3H), 2.98 (s, 3H).

Synthesis of diacetyl-4,4-dimethyl-4'-methylbis(thiosemicarbazone) (2)²⁷

Compound 1 (0.92 g, 5.3 mmol) was dissolved in 3 mL of DMF and reacted with 4,4-dimethyl-3-thiosemicarbazide (0.761 g, 6.4 mmol) in presence of 6 drops of glacial acetic acid at room temperature. After 48 h, the suspension was added dropwise over 60 mL of distilled water at 2 °C, in which an abundant yellow solid precipitated. The suspension was filtered and the solid was washed with cold ethanol and diethyl ether. Compound 2 was obtained as a yellow solid (1.18 g, yield 81 %). ¹H NMR (400.13 MHz, DMSO-*d*₆), δ (ppm): 10.20 (s, 1H), 9.49 (s, 1H), 8.36 (s, 1H), 3.28 (s, 6H), 3.03 (s, 3H), 2.19 (s, 3H), 2.14 (s, 3H).

Synthesis of diacetyl-4-butyric acid-4'-methylbis(thiosemicarbazone) (ATSM(CH₂)₃COOH)²⁷

Compound 2 (0.28 g, 1.0 mmol) and 4-aminobutyric acid (0.22 g, 2.1 mmol) were suspended in 33 mL of acetonitrile. The resulting mixture was refluxed under Ar atmosphere and intense stirring for 41 h. The suspension was then filtered and the resulting solid was washed with HCl 3% (3 × 3 mL), CH₃CN (40 mL) and diethyl ether (3 × 30 mL). ATSM(CH₂)₃COOH was obtained as a white solid (0.16 g, yield 47.1 %). ¹H NMR (400.13 MHz, DMSO-*d*₆), δ (ppm): 12.05 (bb, 1H), 10.22 (s, 1H), 10.17 (s, 1H), 8.43 (s, 1H), 8.37 (s, 1H), 3.59 (s, 2H), 3.03 (s, 3H), 2.25 (s, 2H), 2.21 (s, 6H), 1.81 (s, 2H). ¹³C NMR (500.13 MHz, DMSO-*d*₆), δ (ppm): 178.9, 178.3, 174.7, 148.6, 148.4, 43.7, 31.67, 24.6, 12.2. LC-MS, m/z: Calculated for C₁₁H₂₁N₆O₂S₂: 333.12; Found: [L - H]⁻ 332.99.

I. Figures

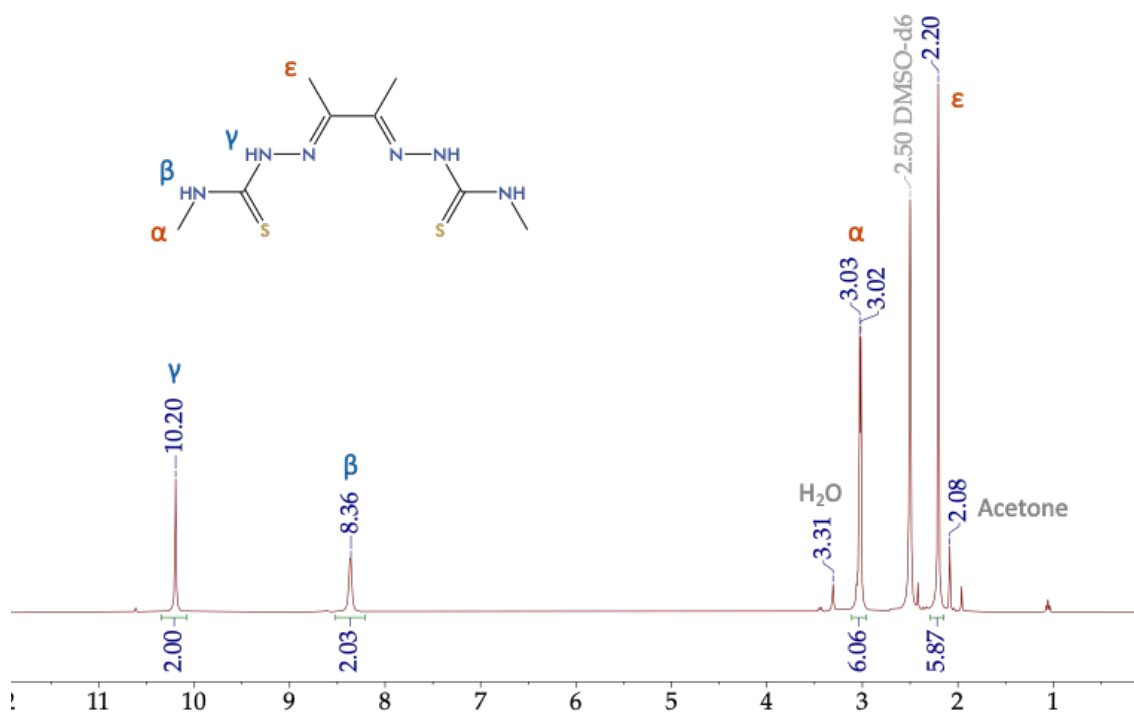


Figure S1. ¹H-NMR spectrum of ATSM in *d*₆-DMSO.

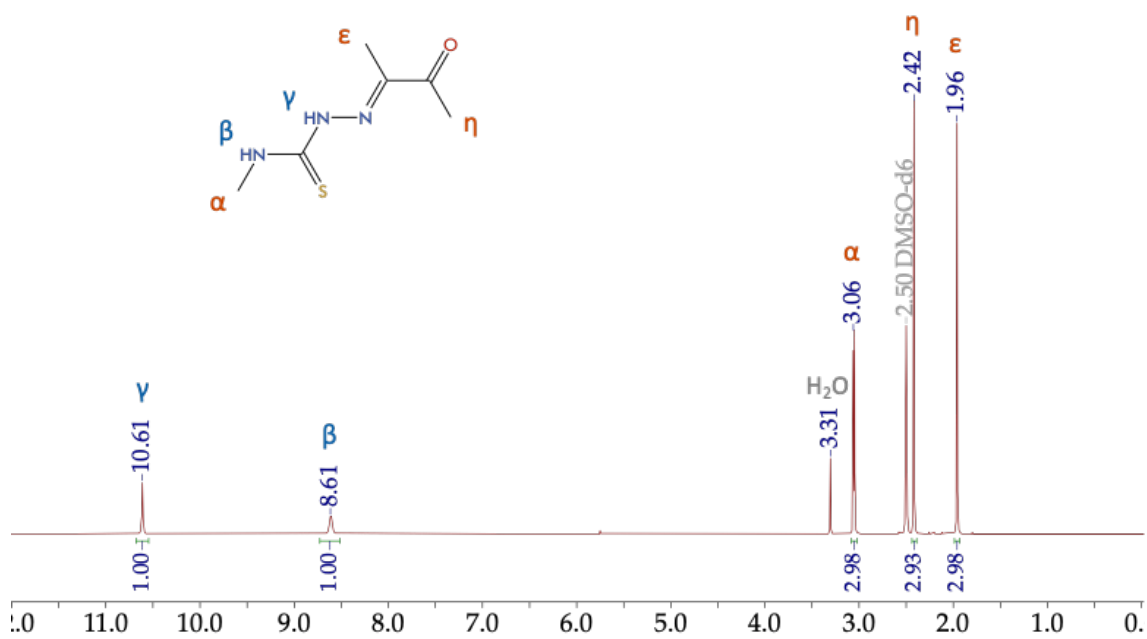


Figure S2. ¹H-NMR spectrum of 1 in *d*₆-DMSO.

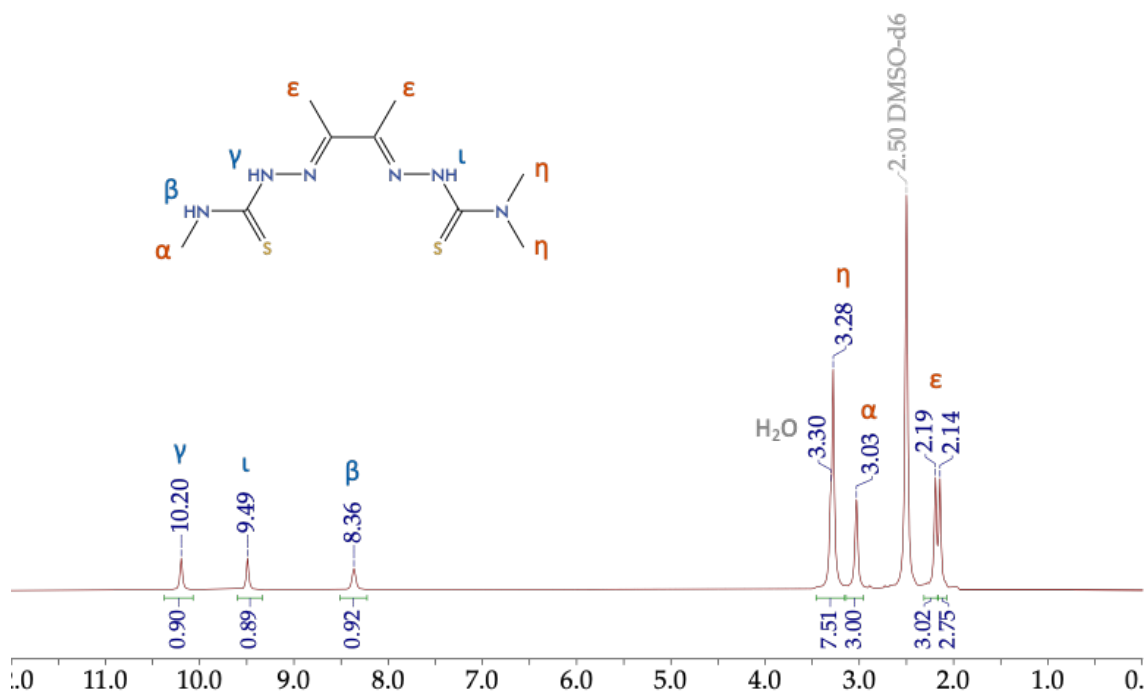


Figure S3. ¹H-NMR spectrum of 2 in *d*₆-DMSO.

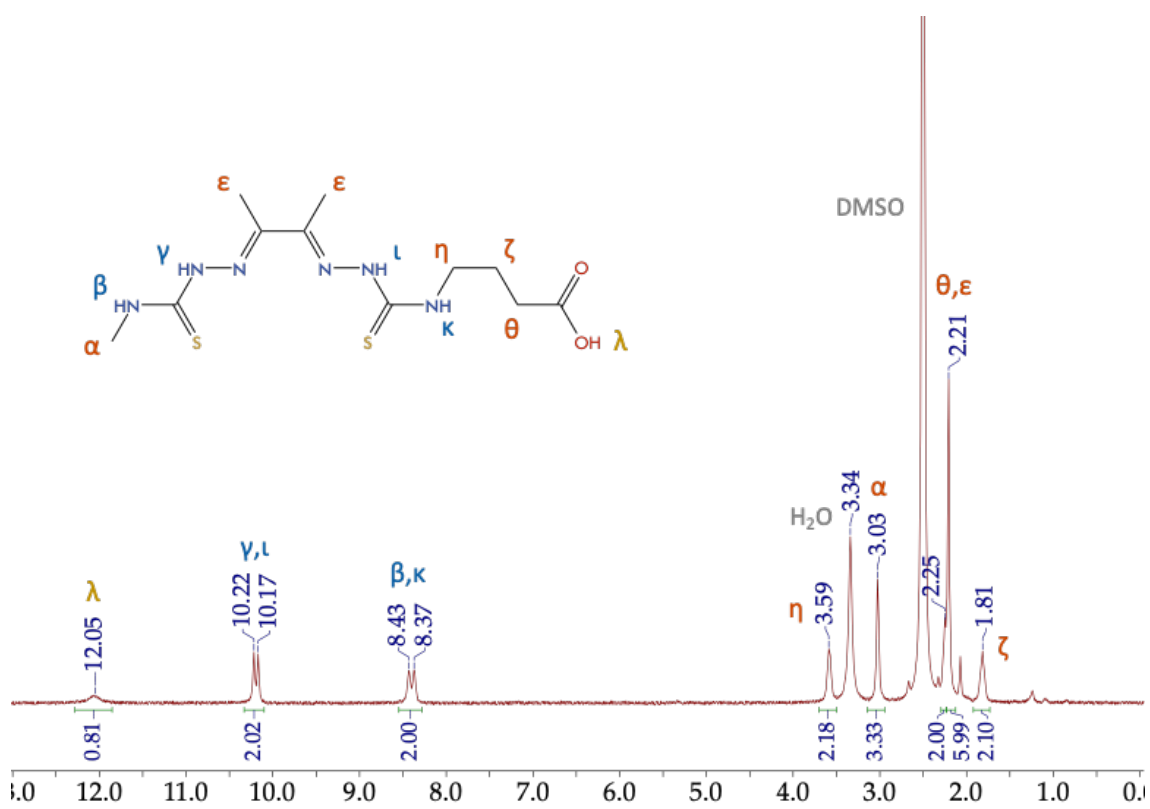


Figure S4. ¹H-NMR spectrum of ATSM(CH₂)₃COOH in *d*₆-DMSO.

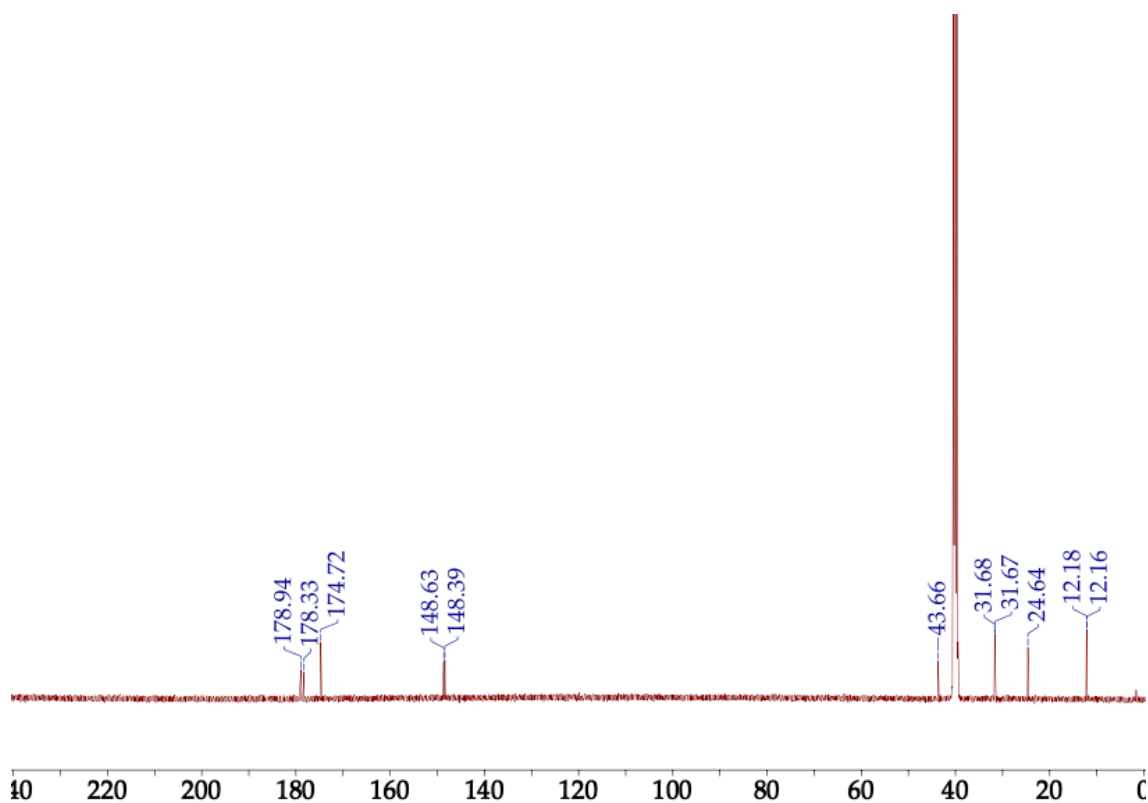


Figure S5. ^{13}C -NMR spectrum of ATSM(CH₂)₃COOH in *d*₆-DMSO.

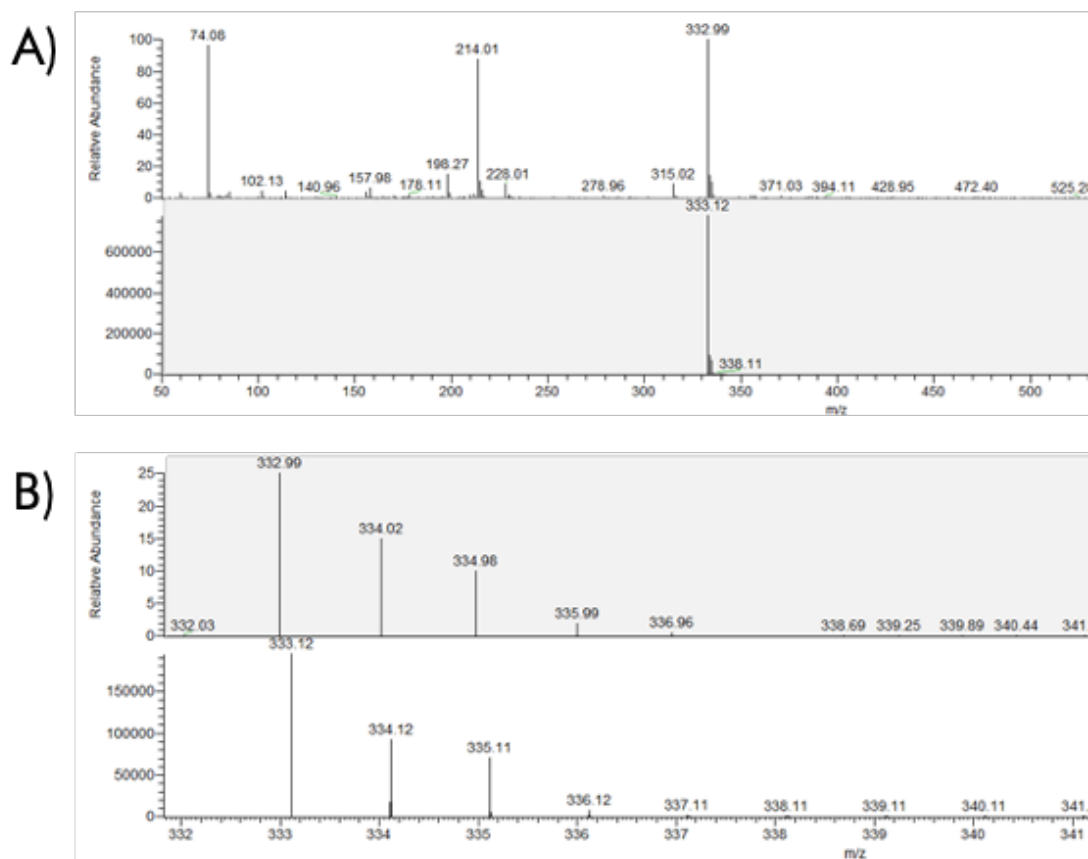


Figure S6. (A) Experimental (top) and theoretical (bottom) LC-MS spectra of ATSM(CH₂)₃COOH. (B) Detail of the experimental (top) and theoretical (bottom) spectra.

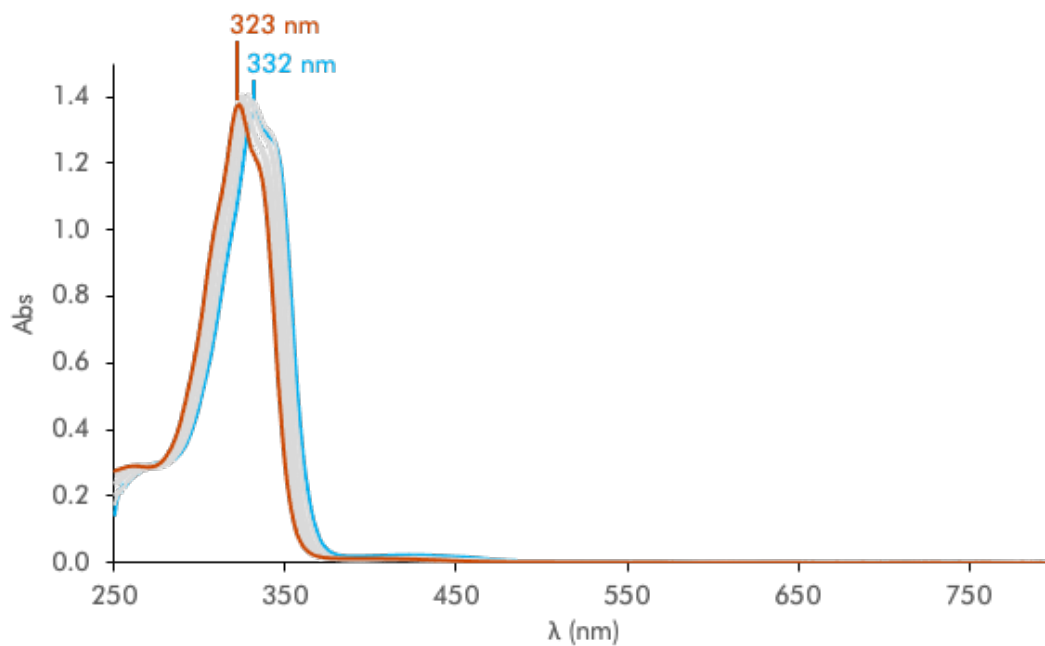


Figure S7. UV-vis spectra of a 30 μM of ATSM in HEPES buffer (pH 7.4, 50 mM) with % of DMSO ranging from 70 (blue) to 0.9 (orange).

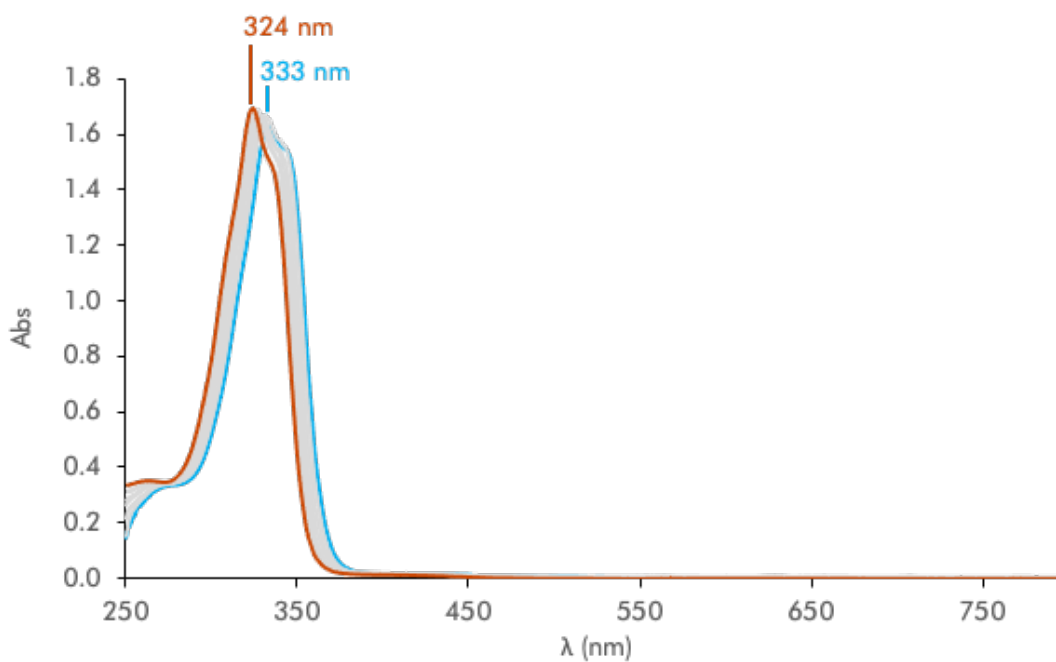


Figure S8. UV-vis spectra of a 30 μM of ATSM(CH₂)₃COOH in HEPES buffer (pH 7.4, 50 mM) with % of DMSO ranging from 75 (blue) to 1.7 (orange).

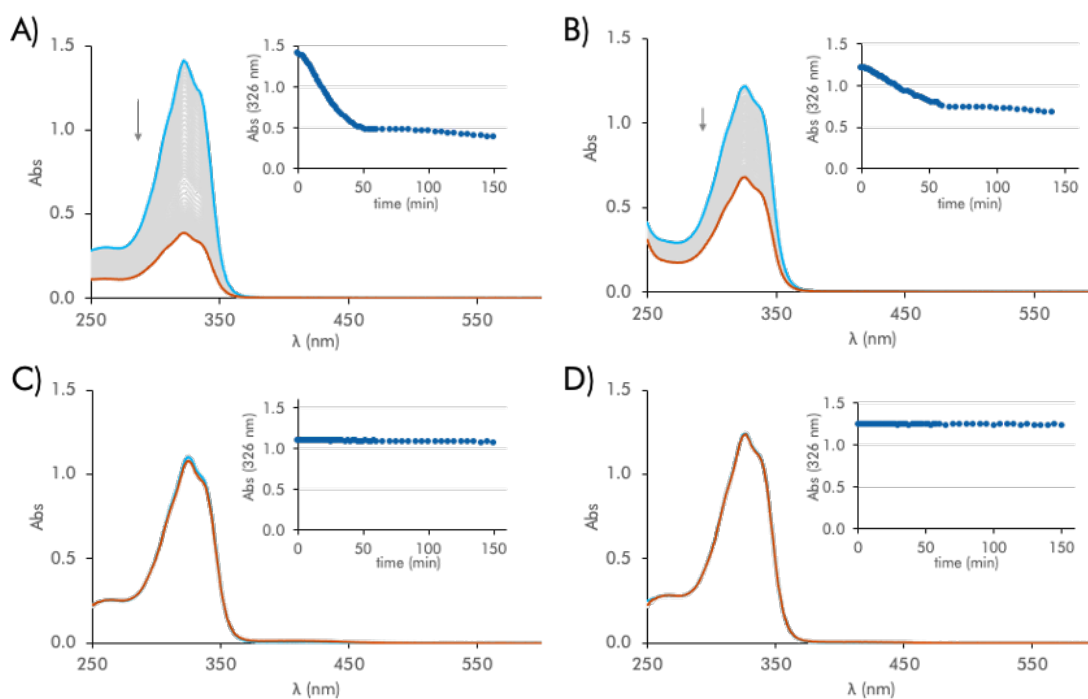


Figure S9. Evolution of the absorbance spectra with time of solutions containing 30 μM of ATSM in HEPES buffer (pH 7.4, 50 mM) with different percentages of DMSO: (A) 1%, (B) 10%, (C) 20% and (D) 30%.

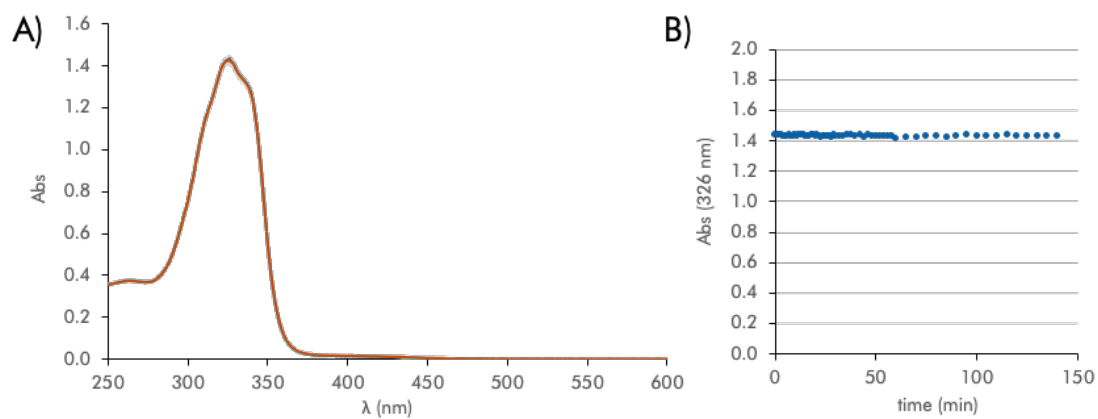


Figure S10. (A) Evolution of the spectra with time of solutions containing 30 μM of ATSM(CH₂)₃COOH and (B) intensity of absorbance at 326 nm in function of time. Medium: HEPES buffer (pH 7.4, 50 mM) with 1% of DMSO.

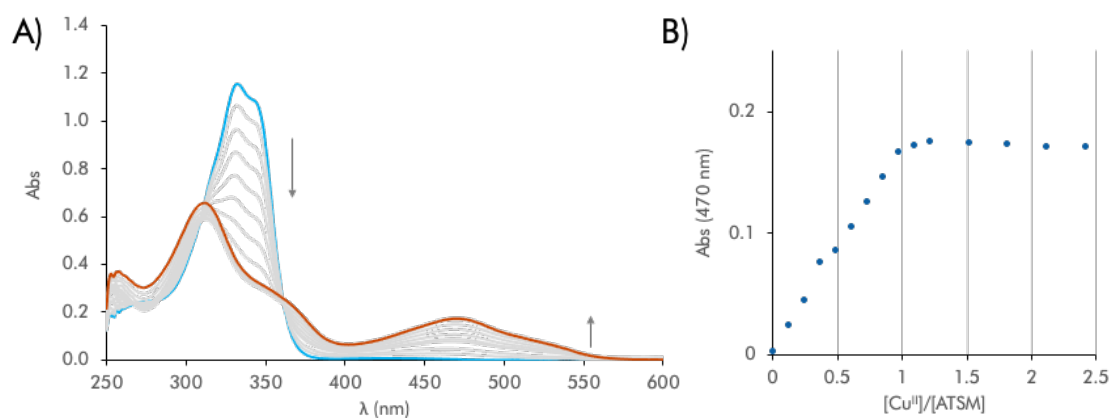


Figure S11. (A) Evolution of the spectra of solutions containing 30 μM of ATSM in HEPES buffer (pH 7.4, 50 mM) and 70% of DMSO upon addition of aliquots of Cu^{II} and (B) representation of the intensity of absorbance at 470 nm of the solutions in function of $[\text{Cu}^{\text{II}}]/[\text{ATSM}]$.

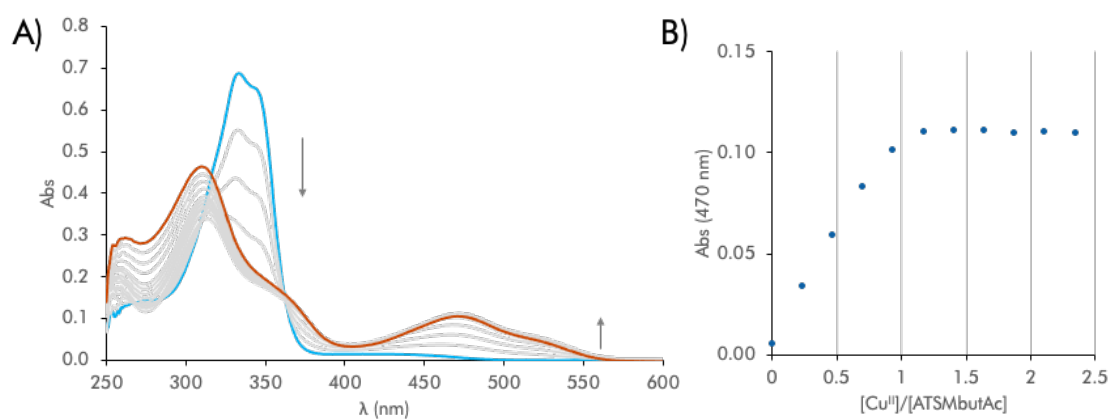


Figure S12. (A) Evolution of the spectra of solutions containing 30 μM of $\text{ATSM}(\text{CH}_2)_3\text{COOH}$ in HEPES buffer (pH 7.4, 50 mM) and 70% of DMSO upon addition of aliquots of Cu^{II} and (B) representation of the intensity of absorbance at 470 nm of the solutions in function of $[\text{Cu}^{\text{II}}]/[\text{ATSM}(\text{CH}_2)_3\text{COOH}]$.

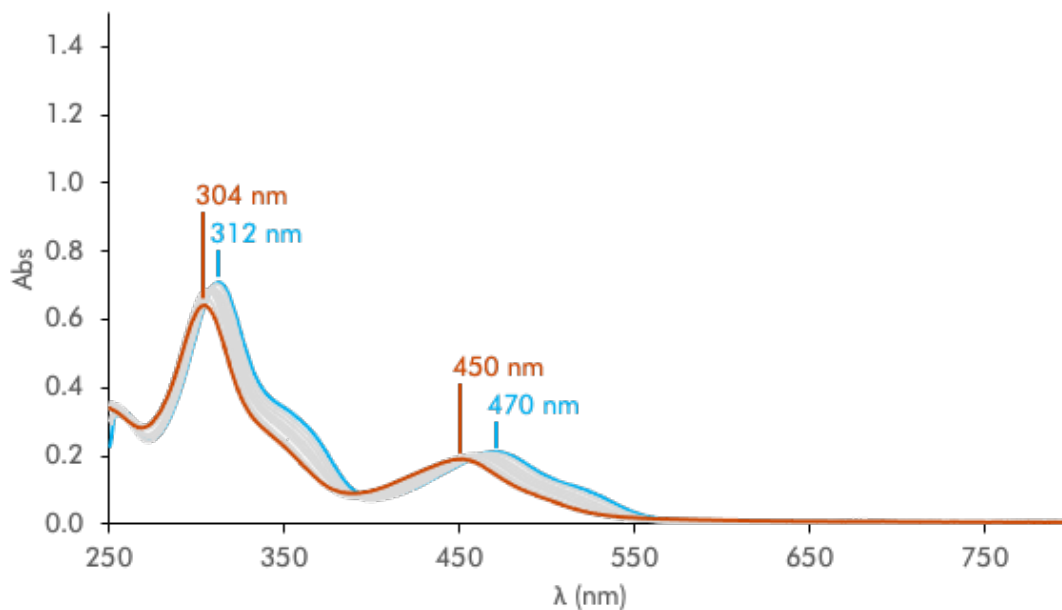


Figure S13. UV-vis spectra of a 30 μM of ATSM in presence of Cu^{II} (1 eq) in HEPES buffer (pH 7.4, 50 mM) with % of DMSO ranging from 70 (blue) to 0.9 (orange).

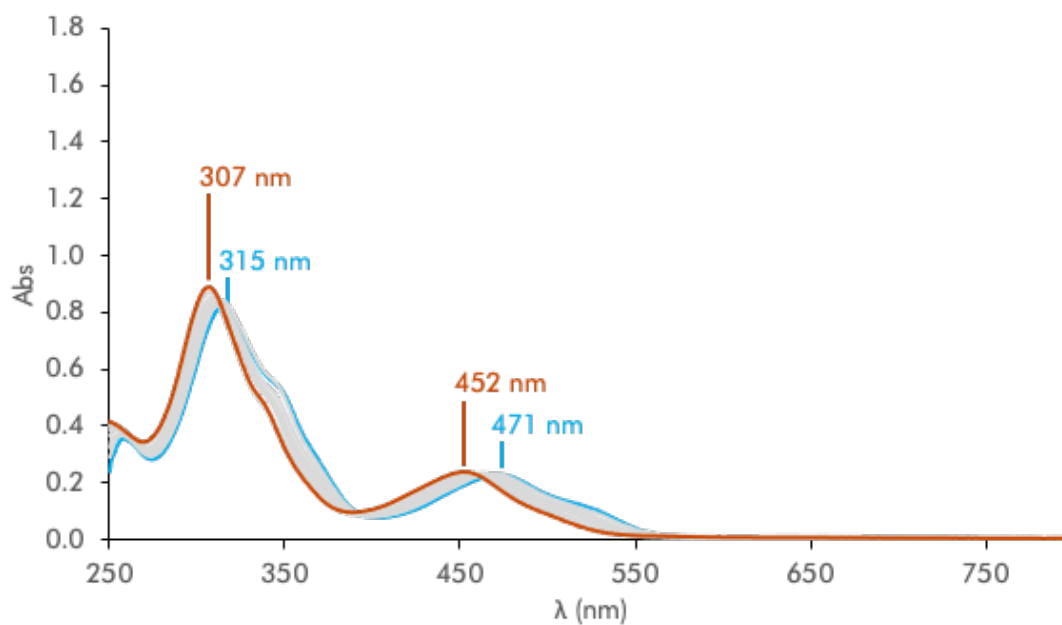


Figure S14. UV-vis spectra of a 30 μM of ATSM(CH₂)₃COOH in presence of Cu^{II} (1 eq) in HEPES buffer (pH 7.4, 50 mM) with % of DMSO ranging from 75 (blue) to 1.7 (orange).

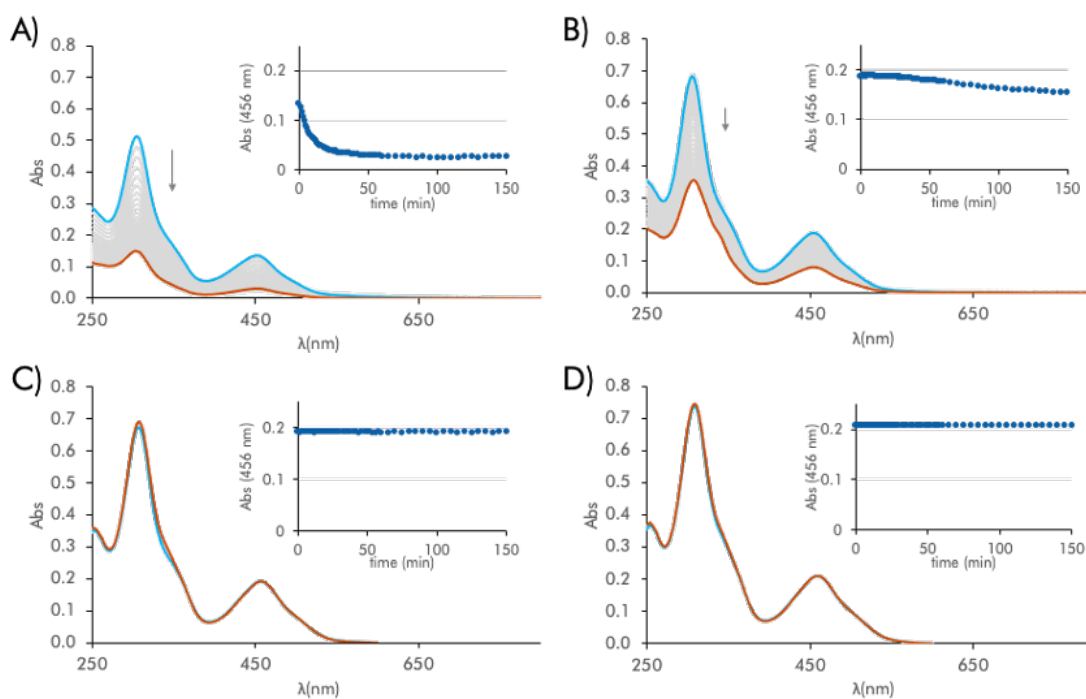


Figure S15. Evolution of the absorbance spectra with time of solutions containing $30 \mu\text{M}$ of ATSM in presence of Cu^{II} (1 eq) in HEPES buffer (pH 7.4, 50 mM) with different percentages of DMSO: (A) 1%, (B) 10%, (C) 20% and (D) 30%. Insets: intensity of absorbance at 456 nm in function of time.

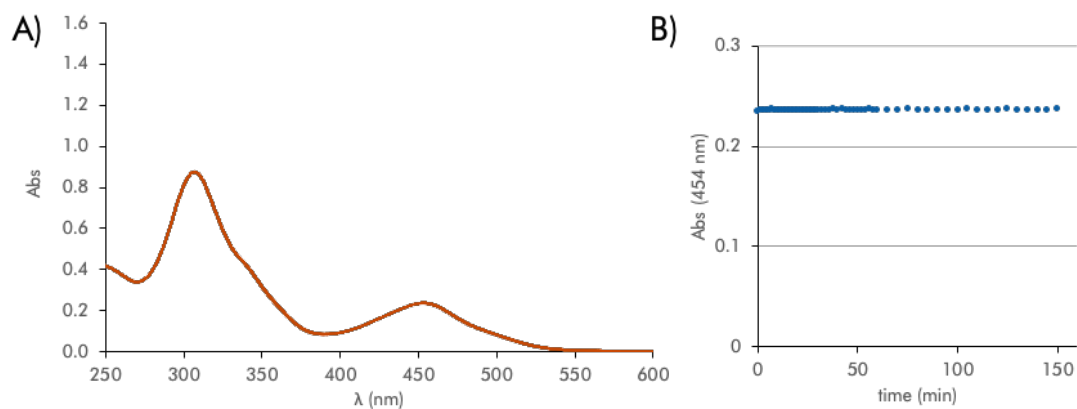


Figure S16. (A) Evolution of the spectra with time of solutions containing $30 \mu\text{M}$ of $\text{ATSM}(\text{CH}_2)_3\text{COOH}$ in presence of Cu^{II} (1 eq) and (B) intensity of absorbance at 454 nm in function of time. Medium: HEPES buffer (pH 7.4, 50 mM) with 1% of DMSO.

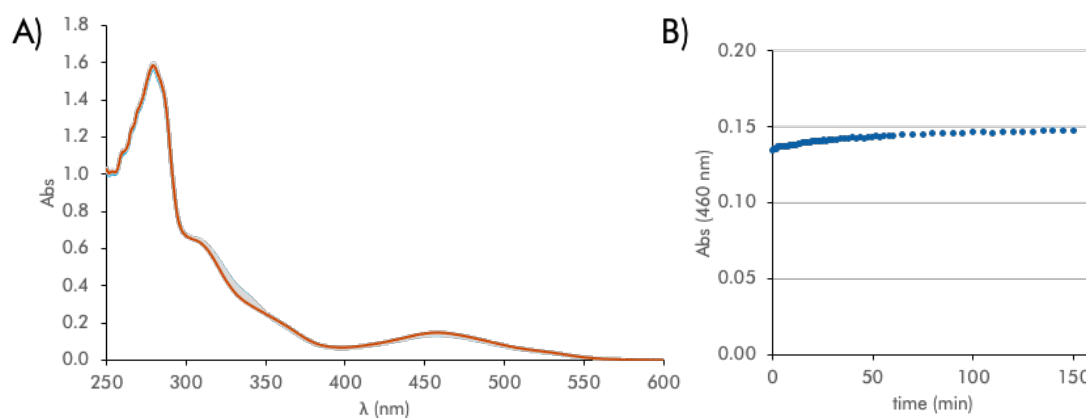


Figure S17. (A) Evolution of the spectra with time of a 30 μM solution of Cu^{II} -ATSM to which 1 eq of HSA was added and (B) intensity of absorbance at 454 nm in function of time. Medium: HEPES buffer (pH 7.4, 50 mM) with 1% of DMSO.

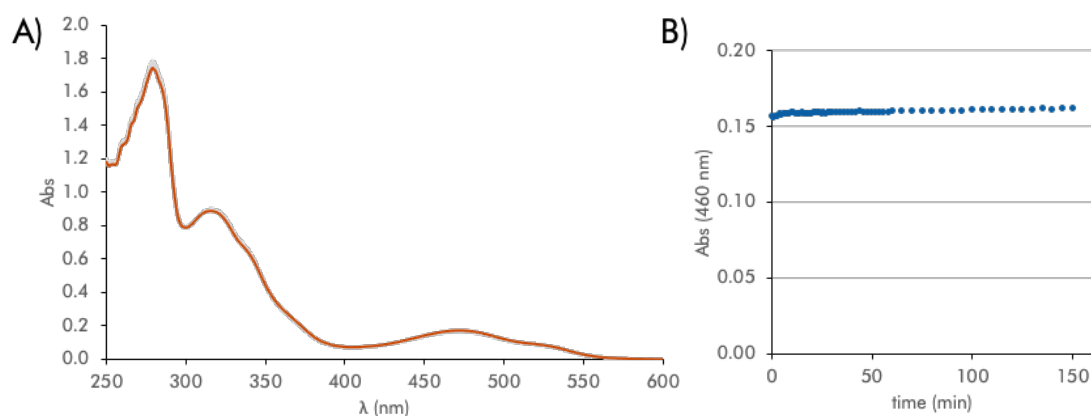


Figure S18. (A) Evolution of the spectra with time of a 30 μM solution of Cu^{II} -ATSM(CH_2) $_3$ COOH to which 1 eq of HSA was added and (B) intensity of absorbance at 460 nm in function of time. Medium: HEPES buffer (pH 7.4, 50 mM) with 1% of DMSO.

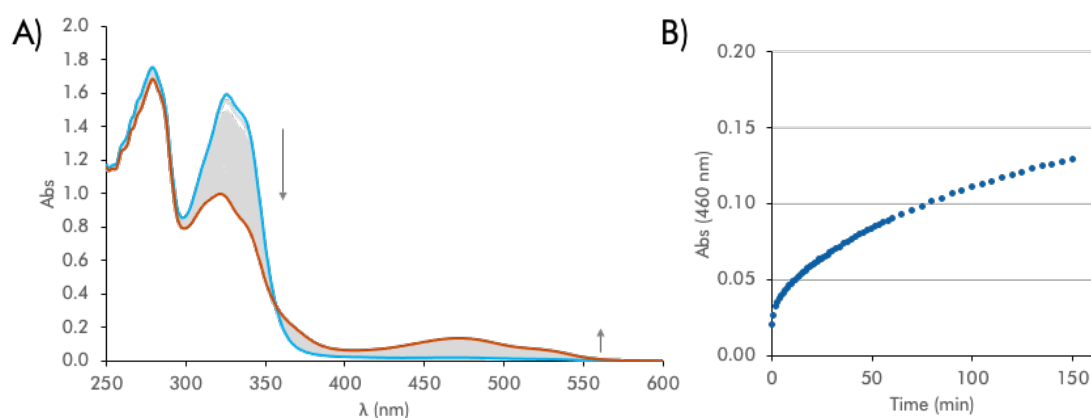


Figure S19. (A) Evolution of the spectra with time of a 30 μM solution of Cu^{II} -HSA to which 1 eq of ATSM(CH_2) $_3$ COOH was added and (B) intensity of absorbance at 460 nm in function of time. Medium: HEPES buffer (pH 7.4, 50 mM) with 1% of DMSO.

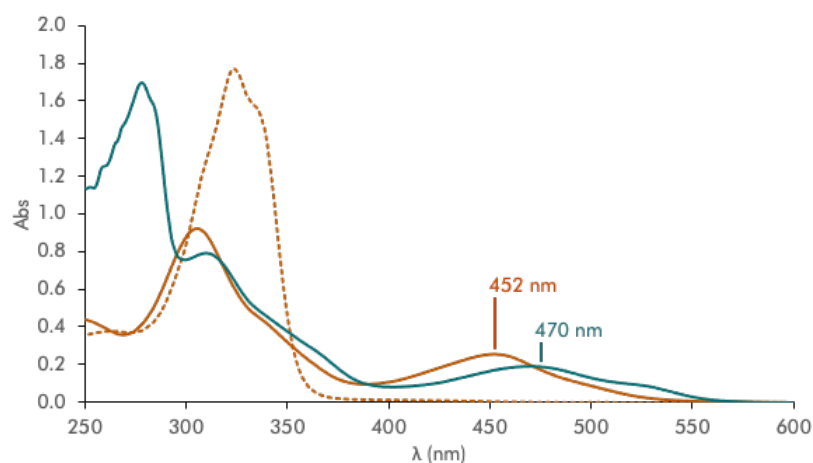


Figure S20. Comparative of the spectra of a 30 μM ATSM(CH₂)₃COOH solution (dotted orange line), a 30 μM ATSM(CH₂)₃COOH solution containing 1 eq of Cu^{II} (in dark orange) and a 30 μM ATSM(CH₂)₃COOH solution containing 1 eq of Cu^{II} and 1 eq of HSA (in dark green).

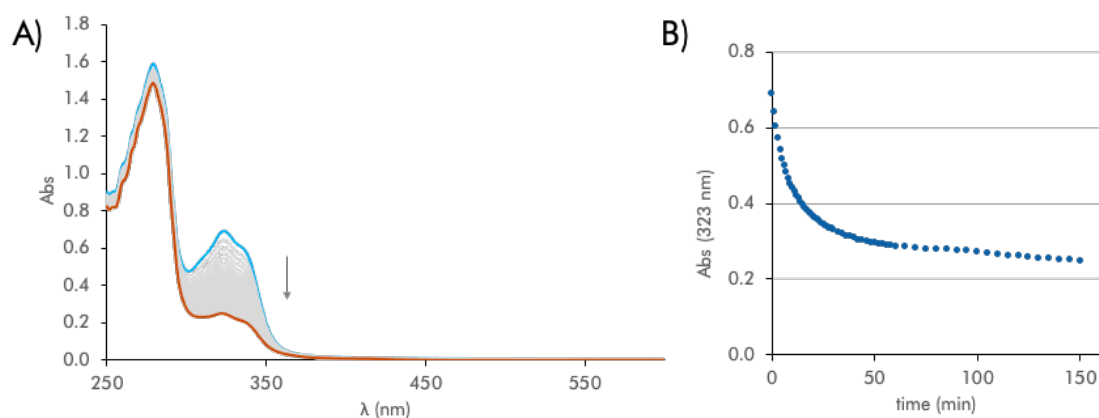


Figure S21. (A) Evolution of the spectra with time of a 30 μM solution of ATSM to which 1 eq of HSA was added and (B) intensity of absorbance at 323 nm in function of time. Medium: HEPES buffer (pH 7.4, 50 mM) with 1% of DMSO.

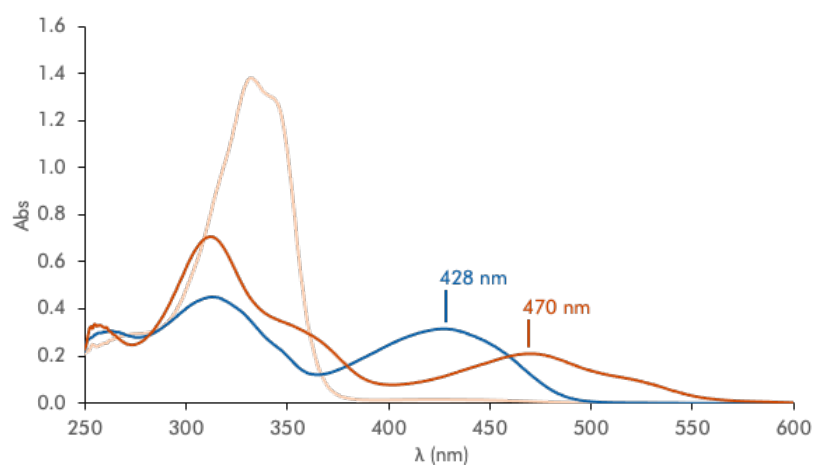


Figure S22. Comparative of the spectra of a 30 μM ATSM solution (in pale orange), in presence of 1 eq of Cu^{II} (in dark orange) or in presence of 1 eq of Zn^{II} (in dark blue). Medium: HEPES buffer (pH 7.4, 50 mM) with 70% of DMSO.

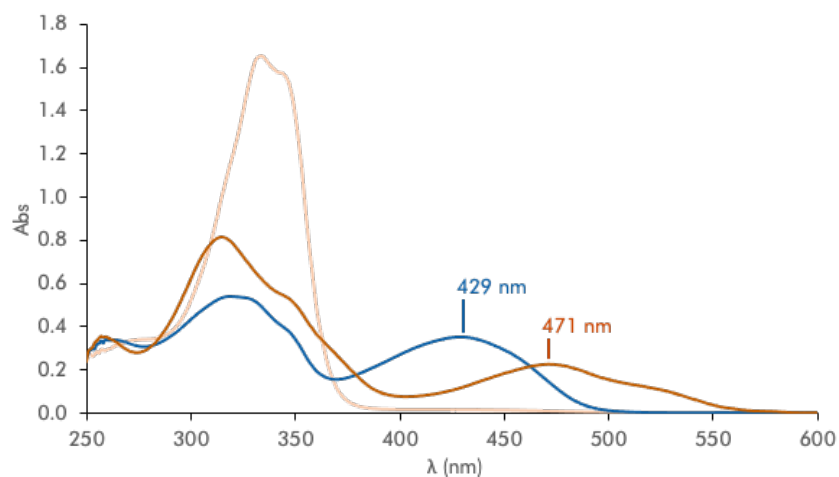


Figure S23. Comparative of the spectra of a 30 μM ATSM(CH₂)₃COOH solution (in pale orange), in presence of 1 eq of Cu^{II} (in dark orange) or in presence of 1 eq of Zn^{II} (in dark blue). Medium: HEPES buffer (pH 7.4, 50 mM) with 70% of DMSO.

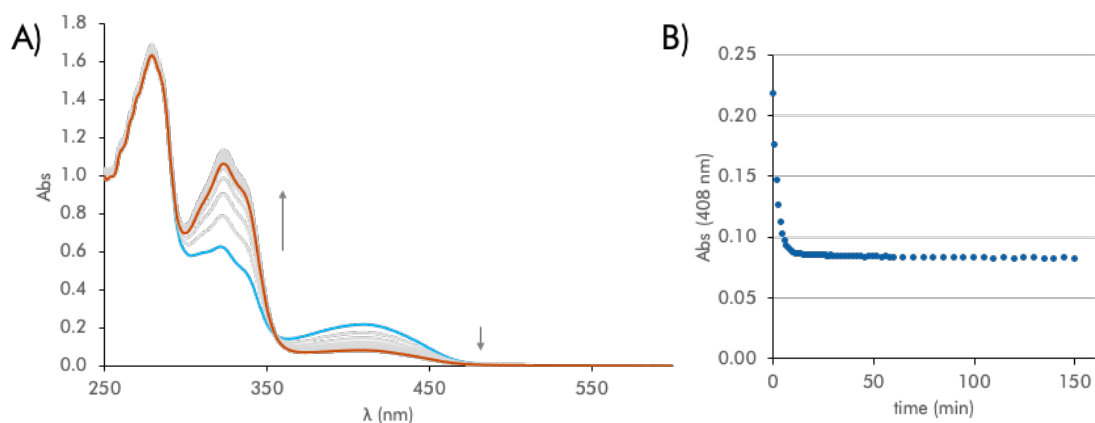


Figure S24. (A) Evolution of the spectra with time of a 30 μM solution of ATSM and Zn^{II} (1:1) after the addition of 1 eq of HSA, (B) intensity of absorbance at 408 nm in function of time. Medium: HEPES buffer (pH 7.4, 50 mM) with 1% of DMSO.

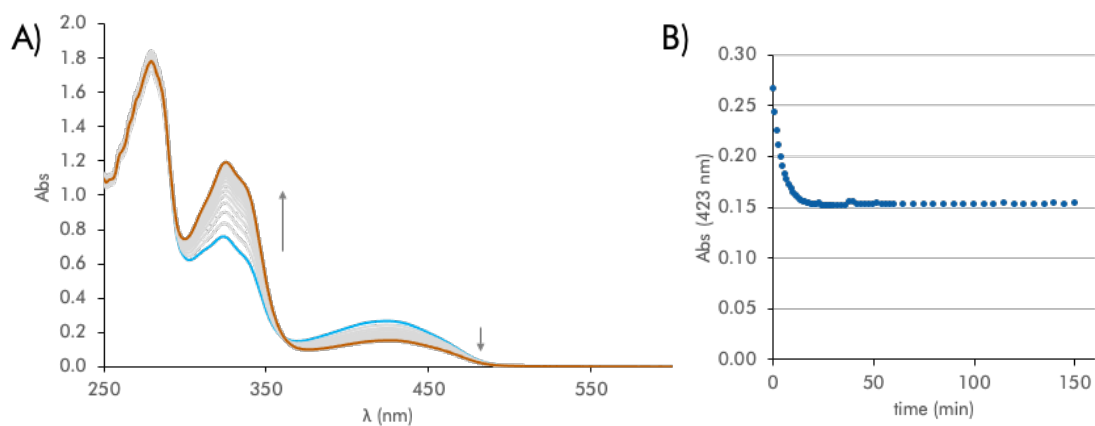


Figure S25. (A) Evolution of the spectra with time of a 30 μM solution of ATSM(CH₂)₃COOH and Zn^{II} (1:1) after the addition of 1 eq of HSA, (B) intensity of absorbance at 423 nm in function of time. Medium: HEPES buffer (pH 7.4, 50 mM) with 1% of DMSO.

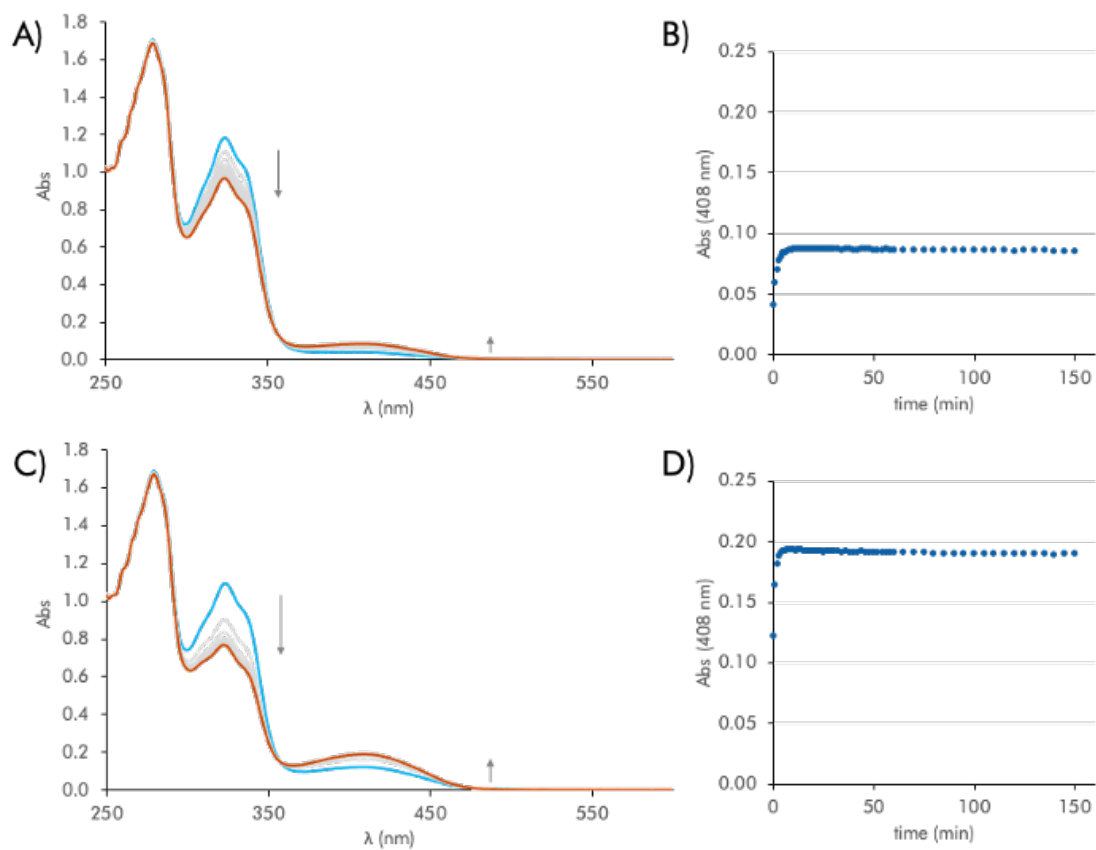


Figure S26. (A) Evolution of the spectra with time of a 30 μM solution of HSA and Zn^{II} (1:1) after the addition of 1 eq of ATSM, (B) intensity of absorbance of this solution at 408 nm in function of time, (C) evolution of the spectra with time of a 30 μM solution of HSA and Zn^{II} (1:2) after the addition of 1 eq of ATSM, (D) intensity of absorbance of this solution at 408 nm in function of time. Medium: HEPES buffer (pH 7.4, 50 mM) with 1% of DMSO.

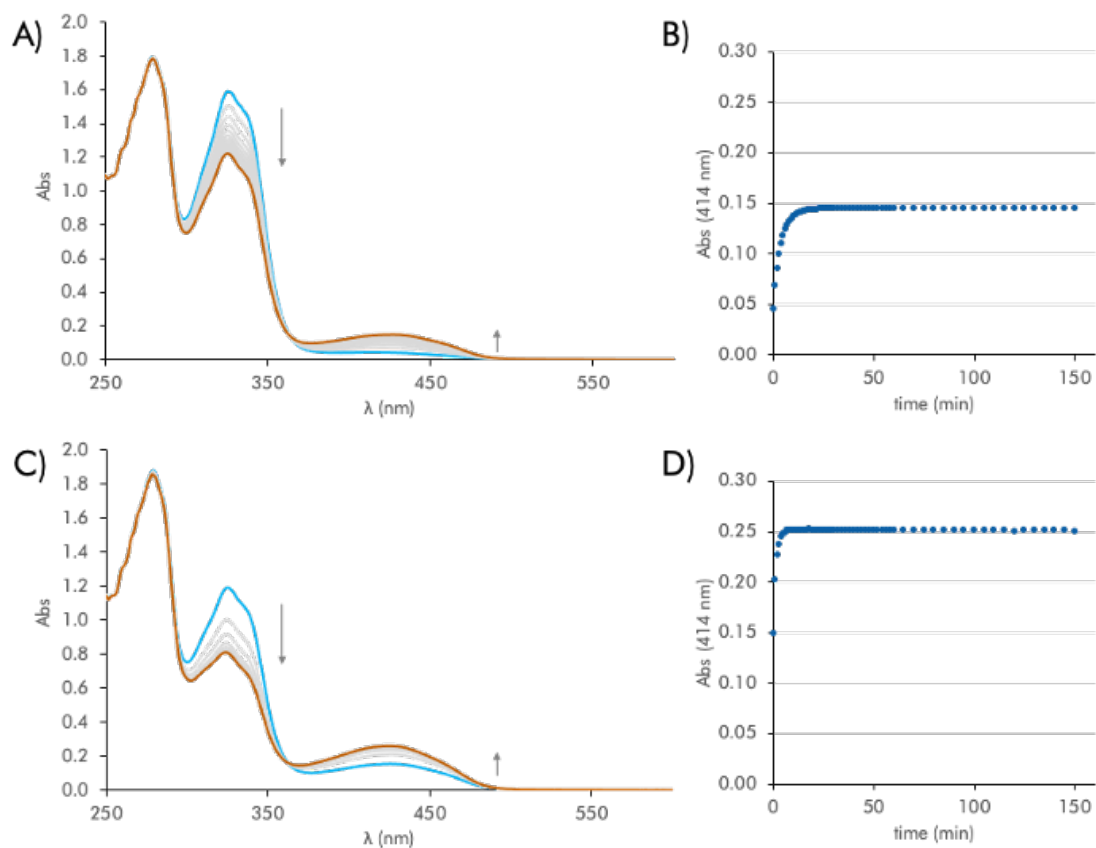


Figure S27. (A) Evolution of the spectra with time of a 30 μ M solution of HSA and Zn^{II} (1:1) after the addition of 1 eq of ATSM(CH₂)₃COOH, (B) intensity of absorbance of this solution at 414 nm in function of time, (C) evolution of the spectra with time of a 30 μ M solution of HSA and Zn^{II} (1:2) after the addition of 1 eq ATSM(CH₂)₃COOH, (D) intensity of absorbance of this solution at 414 nm in function of time. Medium: HEPES buffer (pH 7.4, 50 mM) with 1% of DMSO.

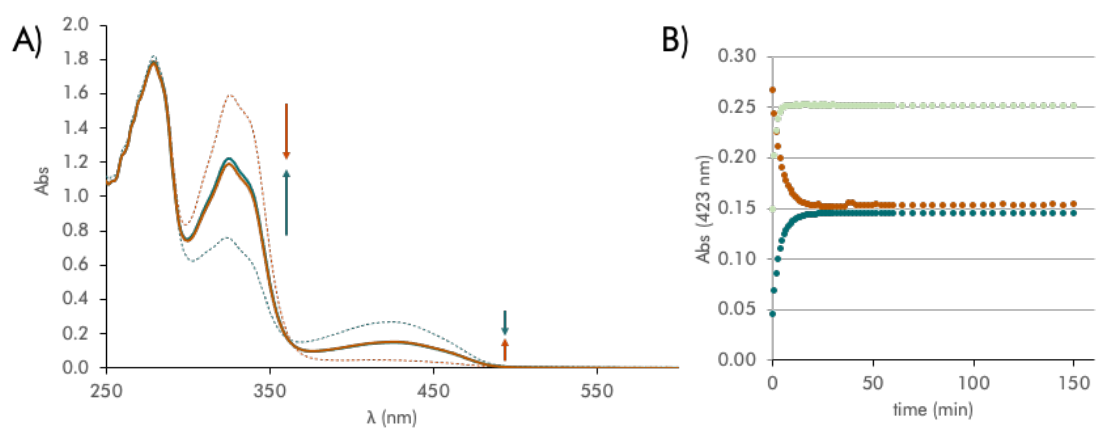


Figure S28. (A) Comparison between the addition of HSA to a solution of Zn^{II}-ATSM(CH₂)₃COOH (orange) and the addition of ATSM(CH₂)₃COOH to a solution of Zn^{II}-HSA (green), [ATSM(CH₂)₃COOH]=[HSA]=[Zn^{II}]=30 μ M, dotted lines correspond to spectra at time 0, and continuous lines correspond to spectra at time 150 min. (B) Intensity of absorbance at 423 nm for the addition of HSA to a solution of Zn^{II}-ATSM(CH₂)₃COOH (orange), the addition of ATSM(CH₂)₃COOH to a solution of Zn^{II}-HSA (1:1) (dark green) and the addition of ATSM(CH₂)₃COOH to a solution of Zn^{II}-HSA (2:1) (pale green). Medium: HEPES buffer (pH 7.4, 50 mM) 1% of DMSO.

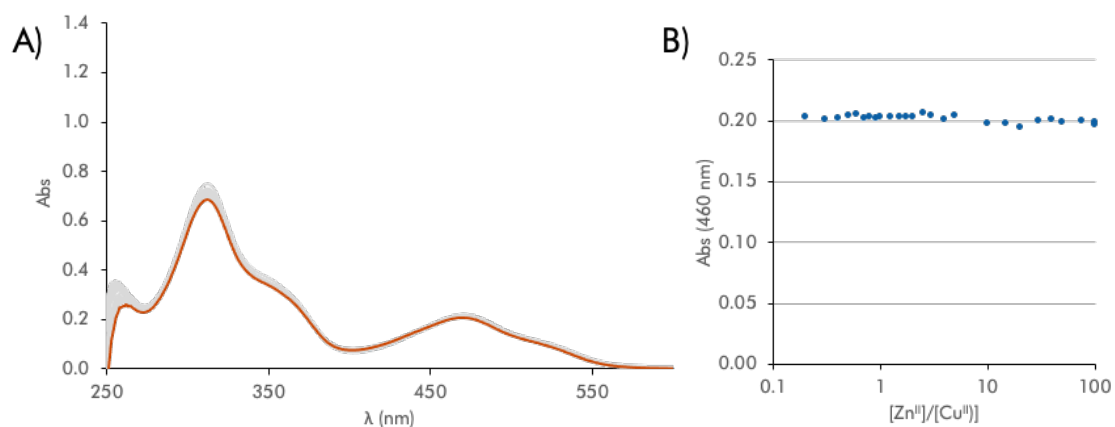


Figure S29. (A) Spectra of a 30 μM solution of Cu^{II} -ATSM after addition of 0.1 to 100 eq of Zn^{II} and (B) intensity of absorbance at 460 nm in function of the equivalents of Zn^{II} (scale in logarithmic units). Medium: HEPES buffer (pH 7.4, 50 mM) with 1% of DMSO.

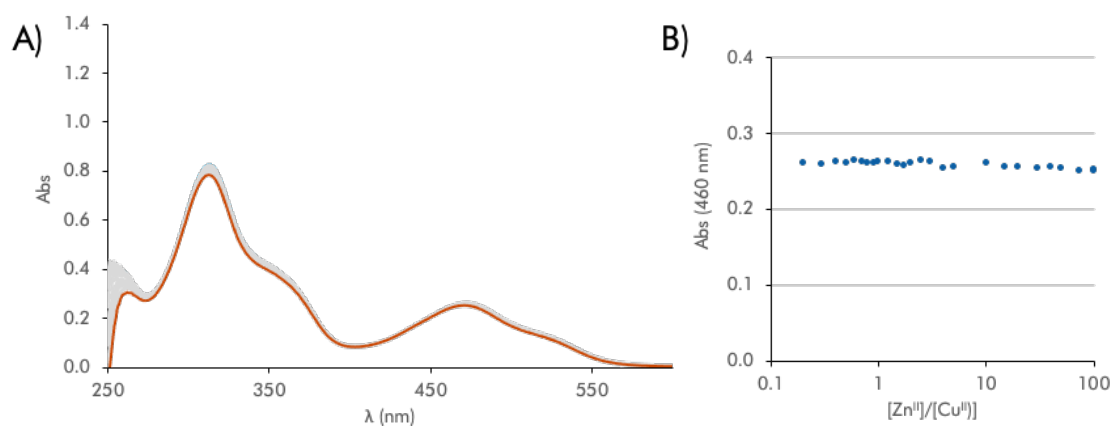


Figure S30. (A) Spectra of a 30 μM solution of Cu^{II} -ATSM(CH_2)₃COOH after addition of 0.1 to 100 eq of Zn^{II} and (B) intensity of absorbance at 460 nm in function of the equivalents of Zn^{II} (scale in logarithmic units). Medium: HEPES buffer (pH 7.4, 50 mM) with 1% of DMSO.

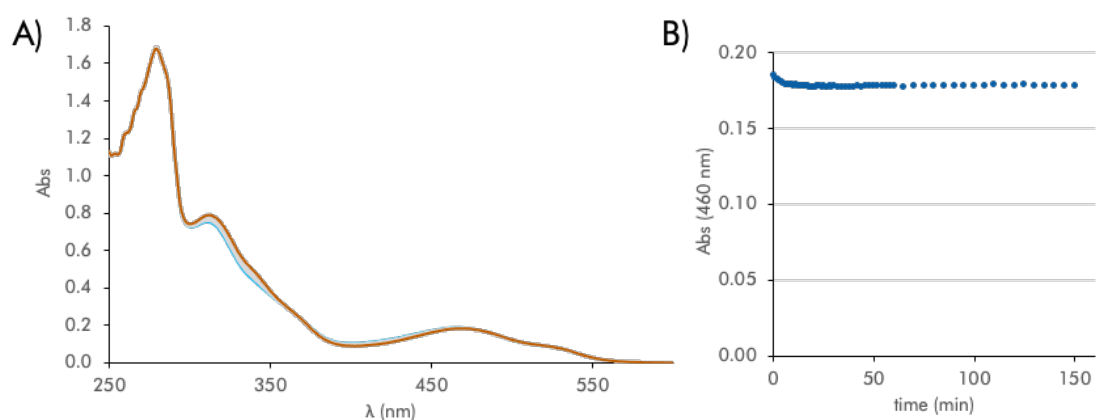


Figure S31. (A) Evolution of the spectra with time of a 30 μM solution of Cu^{II} -ATSM(CH_2)₃COOH after the addition of 1 eq. of HSA and 10 eq. of Zn^{II} , (B) intensity of absorbance at 460 nm in function of time. Medium: HEPES buffer (pH 7.4, 50 mM) with 1% of DMSO.

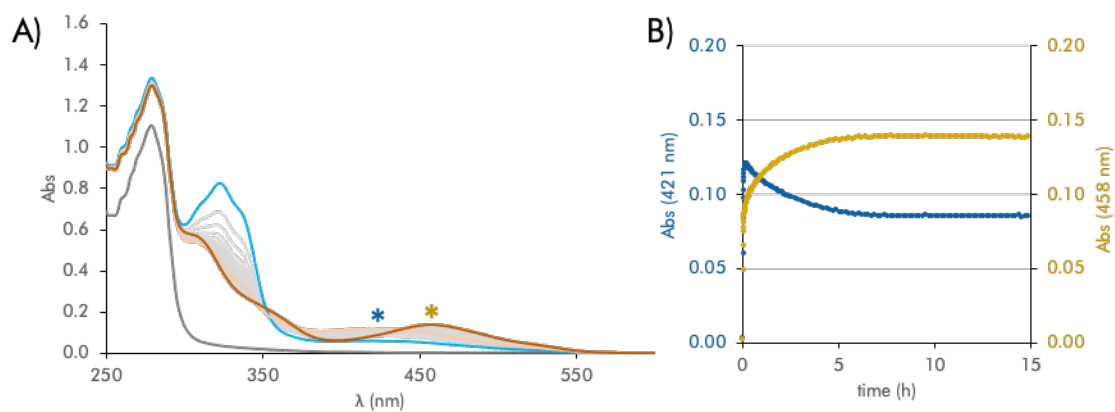


Figure S32. (A) Evolution of the spectra with time of a 30 μM solution of $\text{Cu}^{\text{II}}\text{-Zn}^{\text{II}}\text{-HSA}$ after the addition of 1 eq of ATSM, (B) intensity of absorbance at 421 nm (in blue) and at 458 nm (in yellow) in function of time. Medium: HEPES buffer (pH 7.4, 50 mM) with 1% of DMSO.

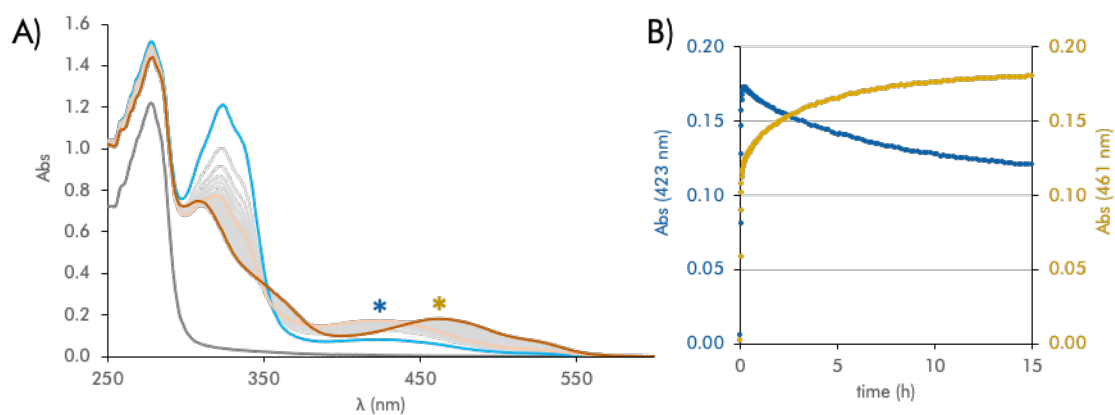


Figure S33. (A) Evolution of the spectra with time of a 30 μM solution of $\text{Cu}^{\text{II}}\text{-Zn}^{\text{II}}\text{-HSA}$ after the addition of 1 eq of $\text{ATSM}(\text{CH}_2)_3\text{COOH}$, (B) intensity of absorbance at 423 nm (in blue) and at 461 nm (in yellow) in function of time. Medium: HEPES buffer (pH 7.4, 50 mM) with 1% of DMSO.

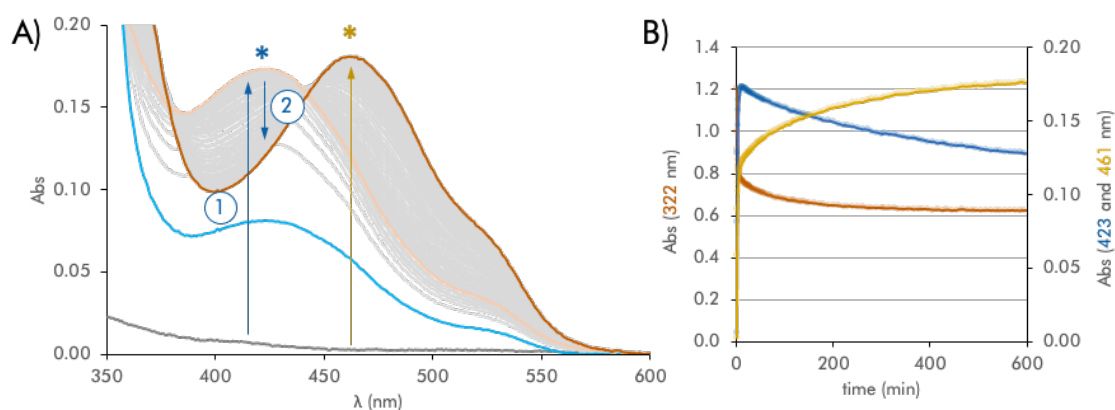


Figure S34. (A) Detail of the evolution of the spectra with time of a 30 μM solution of $\text{Cu}^{\text{II}}\text{-Zn}^{\text{II}}\text{-HSA}$ after the addition of 1 eq of $\text{ATSM}(\text{CH}_2)_3\text{COOH}$, (B) intensity of absorbance of the ligand (322 nm, orange), the Zn^{II} complex (421 nm, blue) and the Cu^{II} complex (458 nm, yellow) in function of time. Medium: HEPES buffer (pH 7.4, 50 mM) with 1% of DMSO.

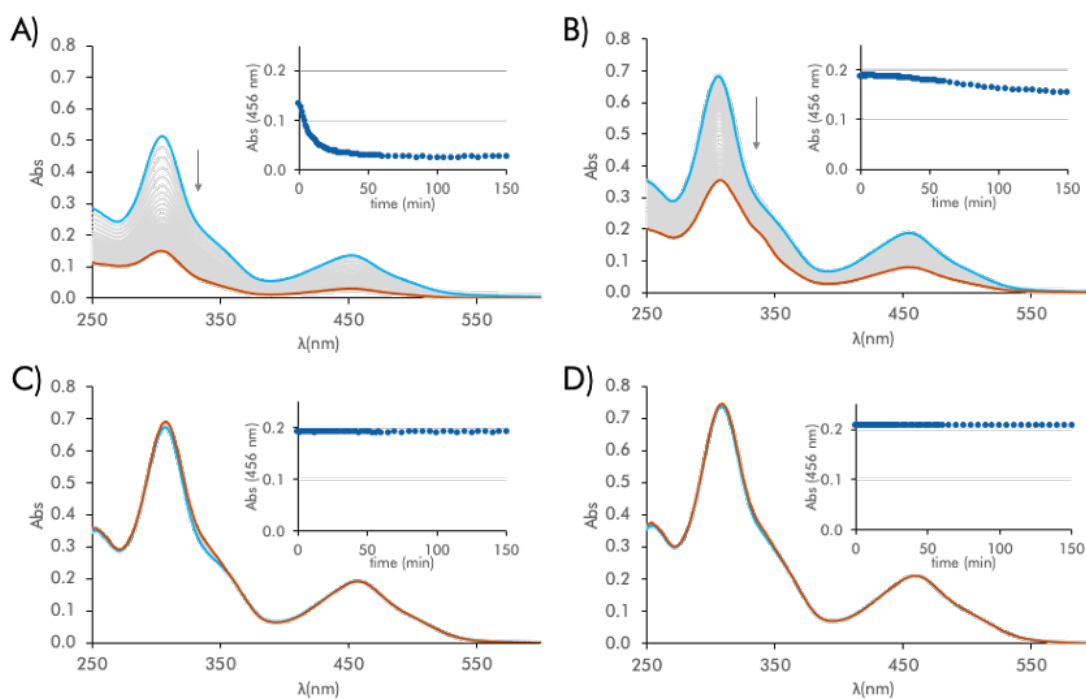


Figure S35. Evolution of the absorbance spectra with time of a 30 μM solution of Cu^{II} -ATSM after the addition of 1 eq. of EDTA in HEPES buffer (pH 7.4, 50 mM) with different percentages of DMSO: (A) 1%, (B) 10%, (C) 20% and (D) 30%.

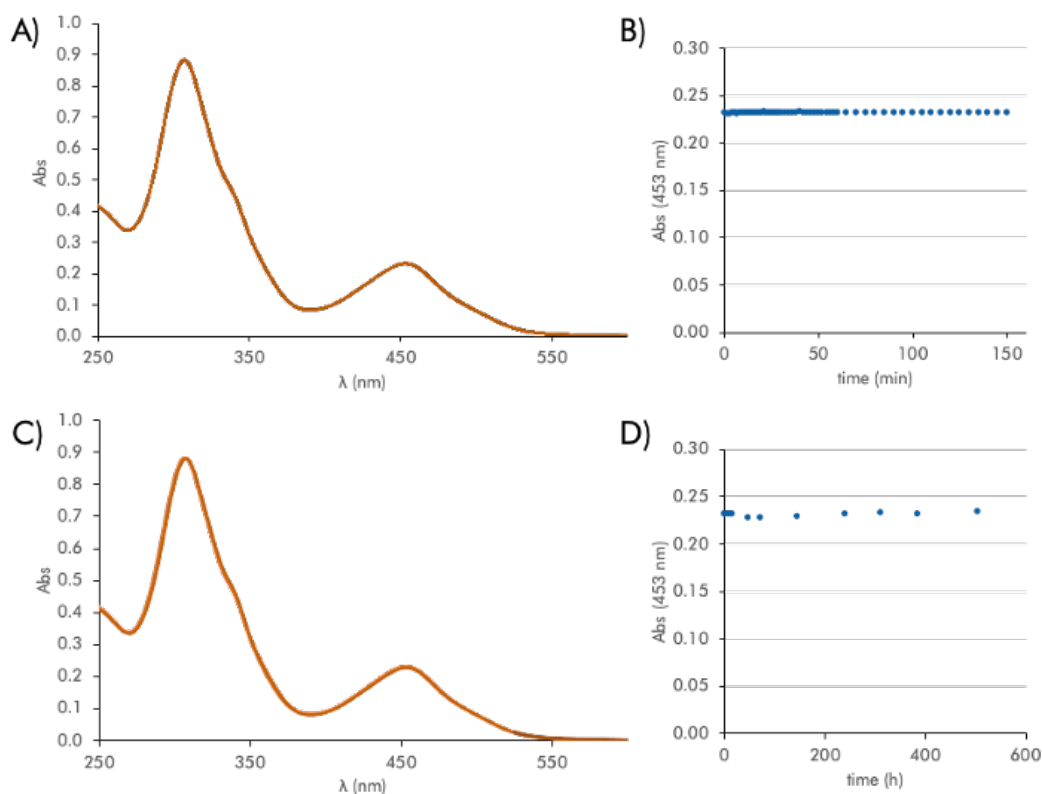


Figure S36. (A) Evolution of the absorbance spectra with time of a 30 μM solution of Cu^{II} -ATSM(CH_2)₃COOH after the addition of 1 eq. of EDTA during 2.5 h, (B) intensity of absorbance of this solution at 408 nm in function of time and (C) and (D) the equivalent measurements carried out during 500 h. Medium: HEPES buffer (pH 7.4, 50 mM) with 1% of DMSO.

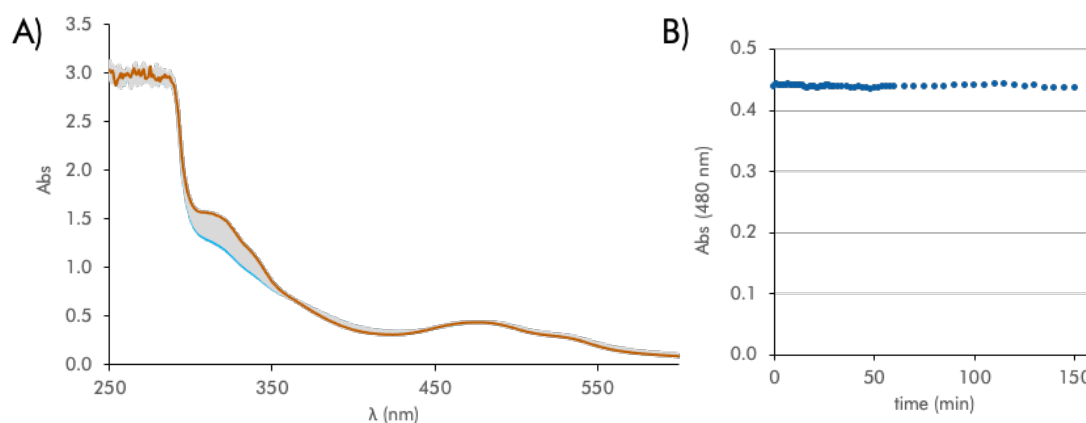


Figure S37. (A) Evolution of the spectra with time of a 30 μM solution of Cu^{II} -ATSM after the addition of 1 eq. of HSA and 1 eq. of EDTA, (B) intensity of absorbance at 480 nm in function of time. Medium: HEPES buffer (pH 7.4, 50 mM) with 1% of DMSO.

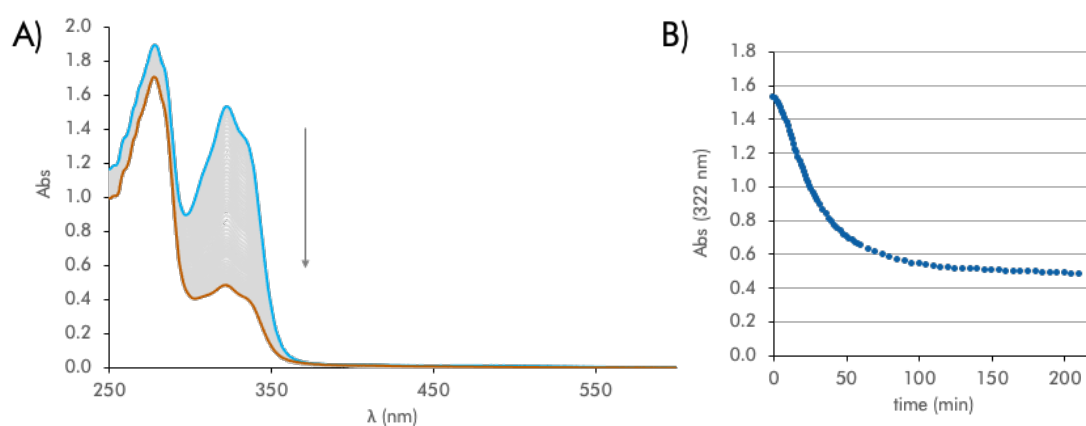


Figure S38. (A) Evolution of the spectra with time of a 30 μM solution of Cu^{II} -EDTA after the addition of 1 eq. of HSA and 1 eq. of ATSM, (B) intensity of absorbance at 322 nm in function of time. Medium: HEPES buffer (pH 7.4, 50 mM) with 1% of DMSO.

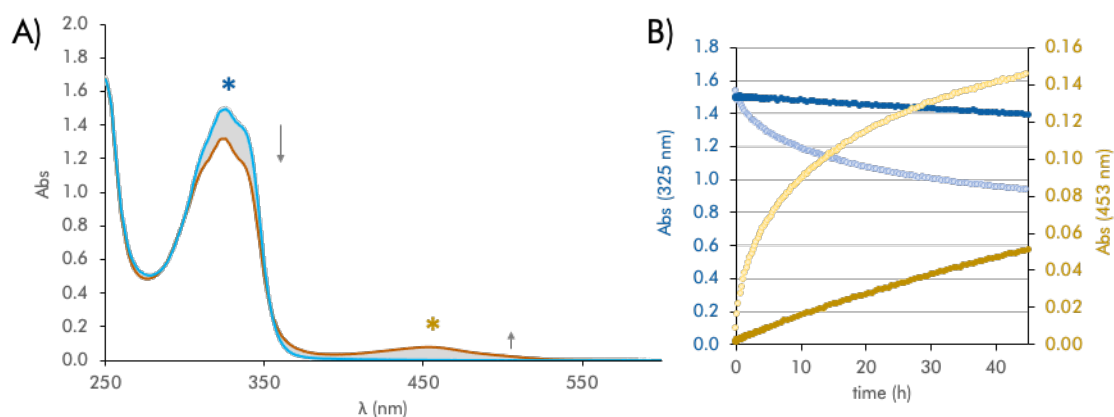


Figure S39. (A) Evolution of the spectra with time of a 30 μM solution of Cu^{II} after the addition of 1,000 eq. of EDTA and then 1 eq. of $\text{ATSM}(\text{CH}_2)_3\text{COOH}$, (B) intensity of absorbance at 325 nm (in blue) and at 453 nm (in yellow) in function of time vs. the competition with 1 eq. of EDTA (325 nm in pale blue and 453 nm in pale yellow). Medium: HEPES buffer (pH 7.4, 50 mM) with 1% of DMSO.

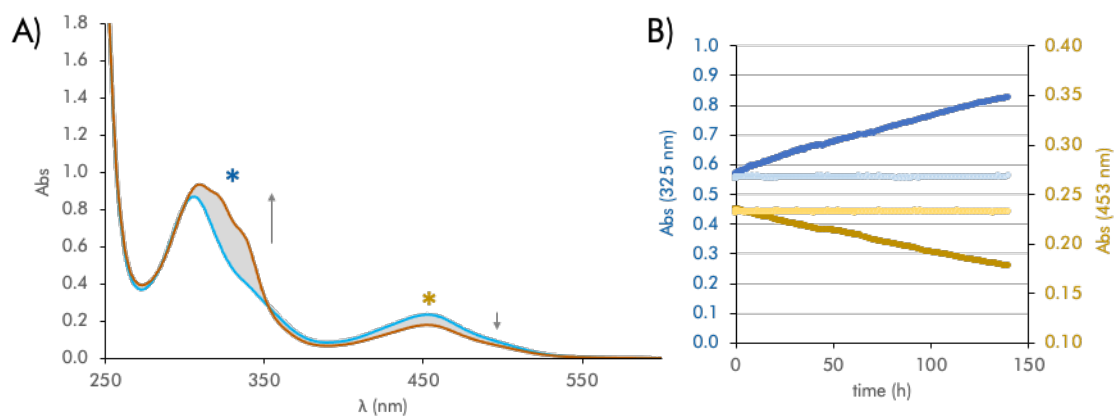
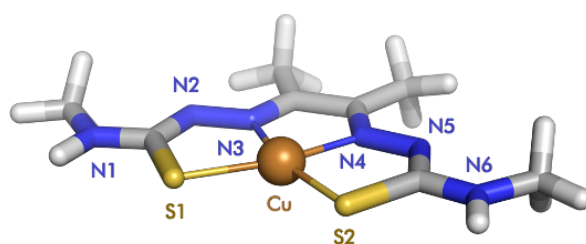


Figure S40. (A) Evolution of the spectra with time of a 30 μM solution of $\text{Cu}^{\text{II}}\text{-ATSM}(\text{CH}_2)_3\text{COOH}$ after the addition of 1,000 eq. of EDTA, (B) intensity of absorbance at 325 nm (in blue) and at 453 nm (in yellow) in function of time vs. the competition with 1 eq. of EDTA (325 nm in pale blue and 453 nm in pale yellow). Medium: HEPES buffer (pH 7.4, 50 mM) with 1% of DMSO.

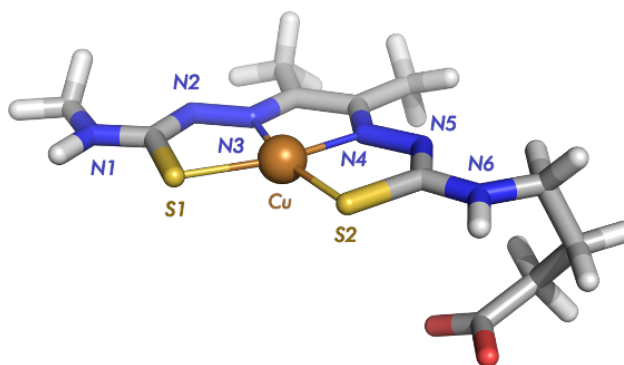
II. Tables

Table 3. Distances and angles in the complex Cu^{II}-ATSM.



Distances (Å)		Angles (°)	
S1-Cu	2.283	S1-Cu-N3	84.6
N3-Cu	2.004	S1-Cu-N4	164.7
N4-Cu	2.004	S1-Cu-S2	110.8
S2-Cu	2.283	N3-Cu-N4	80.1
		N3-Cu-S2	164.7
		N4-Cu-S2	84.6

Table 4. Distances and angles in the complex Cu^{II}-ATSM(CH₂)₃COOH



Distances (Å)		Angles (°)	
S1-Cu	2.286	S1-Cu-N3	84.5
N3-Cu	2.004	S1-Cu-N4	164.7
N4-Cu	2.006	S1-Cu-S2	110.8
S2-Cu	2.274	N3-Cu-N4	80.2
		N3-Cu-S2	164.7
		N4-Cu-S2	84.5

III. References

- (1) Sun, S.-T.; Wang, H.; Huang, D.; Ding, Y.-L.; Zhang, Y.; Song, D.-P.; Zhang, K.-Y.; Pan, L.; Li, Y.-S. Refractive Index Engineering as a Novel Strategy toward Highly Transparent and Tough Sustainable Polymer Blends. *Chinese J. Polym. Sci.* **2020**, *38* (12), 1335–1344 DOI: 10.1007/s10118-020-2439-1.
- (2) Kozma, I. Z.; Krok, P.; Riedle, E. Direct Measurement of the Group-Velocity Mismatch and Derivation of the Refractive-Index Dispersion for a Variety of Solvents in the Ultraviolet. *J. Opt. Soc. Am. B* **2005**, *22* (7), 1479 DOI: 10.1364/JOSAB.22.001479.